Quaternary International 741 (2025) 109893

Contents lists available at ScienceDirect

Quaternary International

journal homepage: www.elsevier.com/locate/quaint

Cold and arid climates experienced by Central European hunter-gatherers at Stránská skála IV during the Last Glacial Maximum

Rhiannon E. Stevens [a,*], Hazel Reade [a], Alexander J.E. Pryor [b], Kerry L. Sayle [c], Jennifer A. Tripp [d], Petr Neruda [e], Zdeňka Nerudová [f], Martina Roblíčková [e], Thomas Higham [g], Jiří Svoboda [h]

[a] Institute of Archaeology, University College London, London, United Kingdom
[b] University of Exeter, Department of Archaeology and History, Exeter, United Kingdom
[c] SUERC, University of Glasgow, East Kilbride, United Kingdom
[d] Department of Chemistry, University of San Francisco, San Francisco, USA
[e] Anthropos Institute, Moravian Museum, Brno, Czech Republic
[f] Centre for Cultural Anthropology, Moravian Museum, Brno, Czech Republic
[g] Department of Evolutionary Anthropology, University of Vienna, Austria
[h] Brno, Czech Republic

ARTICLE INFO

Keywords:
Multi-isotope analysis
Palaeolithic
Palaeoclimate
Collagen
Prey
Ecology
Radiocarbon
Palaeoecology

ABSTRACT

Several studies have argued that human presence in Central Europe during the Last Glacial Maximum (LGM) may have been restricted to brief periods of climate warming. In particular, Greenland Interstadial-2 (GI-2, c.23,300–22,800 BP), a brief warm event recorded in Greenland ice-core stratigraphy, has been associated with human activity at Central European sites such as Kastelhöhle-Nord and Y-Höhle (Switzerland), and Kammern-Grubgraben (Austria). The Epigravettian open air site of Stránská skála IV, a specialized horse hunting site located in Moravia (Czech Republic), purportedly provides further evidence in support of this hypothesis. However, published radiocarbon dates from Stránská skála IV have age ranges too broad for evaluating the relationship between the chronology of occupation and Greenland ice core stratigraphy events, and low pollen abundance at the site means pollen analysis is an uncertain indicator of climatic conditions. Through a new program of radiocarbon dating and stable isotope analysis of the hunted horse remains from Stránská skála IV, we refine the chronology of the site and provide new insights into environmental conditions during human occupation. Bayesian modelling of seven new ultra-filtered AMS dates moves the timing of site occupation back from 22.8 to 21.1 ka cal. BP to 24.1–23.0 ka cal. BP, indicating that site use occurred prior to GI-2. Stable carbon, nitrogen and sulfur bone collagen isotope results suggest that conditions were cool and arid with an open landscape. Tooth enamel oxygen isotope data indicate mean annual air temperatures of 1.2°C (±3.5°C), consistent with climate-modelled temperature estimates for the region during the LGM. Together these data point to human occupation of the site during pronounced cold conditions characterized by temperatures ~8.5°C below the present-day average. Our results demonstrate that human presence in central Europe during the LGM was not confined to brief warm events, adding to a growing body of evidence that early humans could tolerate more extreme climate conditions than previously thought. Perhaps, at certain times in prehistory climate played a less deterministic role in human distribution than is often assumed.

1. Introduction

The Last Glacial Maximum (LGM, c.26,500–19,000 BP) was the period when ice sheets and glaciers were at their maximum extent during the last ice age (Clark et al., 2009). Climate conditions in northern and central Europe during the LGM were cold and arid with mean annual temperatures as much as 15°C lower than present-day (Strandberg et al., 2011; Heyman et al., 2013). Whilst much of Northern Europe was unoccupied by hunter-gatherers during the LGM due to the harsh climatic conditions, archaeological evidence at several sites in

* Corresponding author.
E-mail address: Rhiannon.stevens@ucl.ac.uk (R.E. Stevens).

https://doi.org/10.1016/j.quaint.2025.109893
Received 18 March 2025; Received in revised form 9 June 2025; Accepted 13 June 2025
Available online 1 July 2025

Central Europe indicate human presence during this period (Terberger and Street, 2002; Klein et al., 2021; Lengyel et al., 2021; Škrdla et al., 2021). The scant archaeological record suggests extremely low population densities indicative of seasonal visits by highly mobile groups that spent much of their time in warmer regions, rather than permanent year round settlements (Gamble et al., 2004; Verpoorte, 2004; Maier et al., 2016; Škrdla et al., 2021). Several studies have argued that human presence in central Europe during the LGM may have been restricted to brief periods of climate warming within the LGM, in particular a brief warming event associated with Greenland Interstadial 2 (GI-2, c. 23, 300–22,800 BP) (Terberger and Street, 2002; Terberger, 2013; Rasmussen et al., 2014; Haesaerts et al., 2016; Reade et al., 2020a; Svoboda et al., 2020). However, climatic and environmental reconstructions directly linked to Central European LGM archaeological sites, and at a time scale relevant to human activity, are extremely rare. Furthermore, there are relatively few high-quality chronometric dates from Central European LGM archaeology sites (although see Lengyel et al., 2021). Many of the radiocarbon dates available were obtained with lower-precision conventional radiometric methods, or used pre-treatment protocols that have now been shown to inadequately remove low molecular weight contaminants (Ramsey et al., 2004a; Higham et al., 2006). Newer pre-treatment protocols that include ultrafiltration to remove the low-molecular weight fraction have been shown to be particularly valuable for refining the chronology of Palaeolithic sites (Higham et al., 2006). This method was recently applied to the LGM sites of Kammern-Grubgraben (Layers 2–4), Kastelhöhle-Nord (intermediate horizon) and Y-Höhle, enabling the timing of human occupation to be refined to 23,400–22,800 cal. BP, which closely corresponds with the timing of the GI-2 warming phase, supporting arguments for human presence being restricted to warm intervals (Rasmussen et al., 2014; Haesaerts et al., 2016; Reade et al., 2020a). Based on limited chronological and pollen data, the Epigravettian site of Stránská skála IV has also been offered as evidence of human presence in the Czech Republic during a warm period during the LGM, around 22, 000 cal. BP (Svoboda et al., 2020). However, some discrepancies exist between the radiocarbon dates, making it difficult at present to compare the timing of human activity with individual events in Greenland Ice-core event stratigraphy (Svoboda et al., 2020). Furthermore, the low abundance of the pollen recovered from the site (Svoboda et al., 2020) means the interpretation of warm conditions is poorly evidenced and therefore questionable. Refining the radiocarbon chronology and environmental context of Stránská skála IV is not only valuable for understanding the environmental conditions when humans were active at the site but can also provide a vital insight into environmental constraints on human settlement at the edge of their geographical range during the LGM. Based on radiocarbon dating and stable isotope analysis (carbon, nitrogen, sulfur, and oxygen) of hunted horse skeletal remains, we present a revised chronology and environmental reconstruction for Stránská skála IV.

1.1. *Stránská skála IV site background*

During the LGM the Epigravettian site of Stránská skála IV (Moravia, Czech Republic) sat within a corridor (c. 400 km wide) delimited by the Fenno-Scandian ice sheet to the north and by the glaciated Alps to the south (Ehlers and Gibbard, 2013; Nerudová et al., 2016). The site was discovered at the base of a Jurassic limestone cliff during a rescue excavation (1985–86) linked to the building of a gas pipeline (Svoboda, 1990; Svoboda et al., 1991, 2020). The small Epigravettian lithic assemblage (blades/bladelets, flakes, end scrapers, cores, and chips) recovered from the site was made from a variety of local Moravian and imported Carpathian materials, including rare long-distance imports such as obsidian, radiolarite and radiolarian chert (Svoboda et al., 2020). No living units or evidence of fire were detected during the excavations; however, 3363 animal osteological specimens were recovered from the site (Boriová et al., 2020). Analysis of the osteological specimens revealed the faunal assemblage was dominated by horse (*Equus ferus*), with reindeer (*Rangifer tarandus*), woolly rhinoceros (*Coelodonta antiquitatis*), and auroch/bison (*Bos/Bison*) also present (Boriová et al., 2020). However, all species except horse (MNI = 10) were represented by a single individual (MNI = 1) (Boriová et al., 2020; Svoboda et al., 2020). On the basis of the characteristic representation of skeletal parts, the site is interpreted to be a specialized horse hunting/butchery site, with some body parts being transported away to camps/different locations (Svoboda, 1990; Svoboda et al., 1991, 2020). Two main accumulations of fauna and artefacts were identified within the excavated area, suggesting the site was used on more than one occasion (Svoboda et al., 2020). The geographic setting of the site likely made it a favourable hunting spot, with the cliff face playing a role in the hunting strategy, either by driving the animals from the plateau over the cliff or driving them from valley bottom upwards and trapping them against cliff face (Svoboda et al., 2020).

The recovery of pollen from the site was limited despite numerous samples being taken (Svoboda et al., 2020). The pollen assemblage is dominated by tree species such as birch (*Betula*) rather than herbs, and includes thermophilic species such as hazel (*Corylus*) and lime (*Tilia*) (Svoboda et al., 2020). It has been suggested that this may indicate the site was used during a brief warm period soon after the LGM, but it has also been highlighted that the thermophilic elements of the pollen assemblage may represent small relic populations surviving locally in a sheltered part of the landscape under generally cold and arid continental climate conditions. Such situations have been observed in contemporaneous records from the western Carpathians and in more recent records from southern Siberia, where climate conditions analogous to those in LGM Central Europe exist today (Jankovská and Pokorný, 2008; Novák et al., 2014; Svoboda et al., 2020). Further, it is also possible that some of the pollen recovered was transported long distances from warmer regions, or may have been reworked from older deposits (Svoboda et al., 2020). Thus, the interpretation of warm conditions during human presence is somewhat circumspect and further environmental information that is linked to the archaeological evidence is needed.

Five prior radiocarbon dates from bone/tooth collagen extracted from the hunted horse remains suggest that site was used during the LGM between 23,750 and 21,100 cal. BP (Lengyel et al., 2021). We argue here that two of those dates (GrN-14351 and GrN-13954: Table 1), made by conventional radiocarbon dating without an ultra-filtration pre-treatment, should be disregarded. Given that the ages obtained from these two samples are younger than the three ultra-filtered Accelerator Mass Spectrometry (AMS) dated samples (DeA-20210, DeA-20212 and Poz-101463, Table 1), it seems likely that the pre-treatment protocol used for GrN-14351 and GrN-13954 may have failed to adequately remove modern contaminants. The three ultra-filtered AMS radiocarbon dates, all from horse teeth, date the site from 23,750 to 22,300 cal. BP which broadly coincides with the brief warming associated with Greenland Interstadial 2 (GI-2: c. 23,290 ± 596 BP to 22,850 ± 573 BP (Rasmussen et al., 2014). The uncertainties associated with these dates are, however, relatively large, thus the calibrated age ranges are too broad to test whether human presence at Stránská skála IV was restricted to GI-2. Two of these teeth (DeA-20210, DeA-20212) were covered with epoxy resin during sampling for strontium isotope analysis (György Lengyel pers. comm.). The resin was removed mechanically prior to sampling for radiocarbon dating (Mihaly Molnar from HEKAL AMS Laboratory pers. comm.). It is also possible that the third tooth may have been treated with PVA glue. While PVA glue was not applied systematically to the faunal material from the site, it was applied occasionally where it was necessary to stabilize the specimen (Sandra Sázelová pers. comm.). Thus, questions remain as to whether the dating of the site could be refined and improved by the dating of clean, previously untreated material. Here we undertake new AMS radiocarbon dating of untreated bones to refine the chronology of the site and stable isotope analyses of horse bones and teeth to

Table 1
Published radiocarbon dates from Stránská skála IV.

^{14}C lab code	^{14}C date	^{14}C uncertainty	Calibrated 14C date BP at 95 % confidence interval	Material	Reference	Comment
GrN-14351	17,740	90	21,890-21100	Bone (Species not given)	Svoboda et al., 1991	Not ultrafiltered during pre-treatment Conventional date.
GrN-13954	18,220	120	22,410-21920	Bone (Species not given)	Svoboda et al., 1991	Not ultrafiltered during pre-treatment Conventional date.
DeA-20212	18,640	130	22,920–22,340	Horse tooth	Svoboda et al. (2020)	Ultrafiltered during pre-treatment. Covered in resin preservative that was removed manually before dating. AMS date.
Poz-101463	18,670	110	22920–22380	Horse tooth	Lengyel et al. (2021)	Ultrafiltered during pre-treatment. May or may not have been conserved with PVA glue. AMS date.
DeA-20210	19,030	250	23,740–22,420	Horse tooth	Lengyel et al. (2021)	Ultrafiltered during pre-treatment. Covered in resin preservative that was removed manually before dating. AMS date.
OxA-V-3079-31	19,375	63	23,740–23,060	Horse bone	This study	Ultrafiltered
OxA-V-3079-32	19,441	32	23,750–23,170	Horse bone	This study	Ultrafiltered
OxA-V-3079-33	19,532	65	23,790–23,300	Horse bone	This study	Ultrafiltered
OxA-V-2776-23	19,560	80	23,800–23,300	Horse bone	This study	Ultrafiltered
OxA-V-3079-35	19,787	66	23,980–23,440	Horse bone	This study	Ultrafiltered
OxA-V-3079-34	19,802	66	24,040–23,470	Horse bone	This study	Ultrafiltered
OxA-V-3079-30	19,884	64	24,120–23,770	Horse bone	This study	Ultrafiltered

reconstruct the environmental conditions experienced by the Epigravettian hunter-gatherers.

1.2. Stable isotopes background

Stable isotope analyses of the archaeological remains of hunted fauna (eg. bones, teeth) are established methods for reconstructing faunal palaeoecology and palaeoenvironmental conditions at the time humans were active within the landscape e.g. (Hedges et al., 2004; Stevens et al., 2009b, 2014; Reade et al., 2016; Drucker et al., 2018; Jones et al., 2019; Pederzani et al., 2021a, 2021b; Britton et al., 2023; Pryor et al., 2024 See review by Stevens et al. 2025a). Carbon (δ^{13}C), nitrogen (δ^{15}N) and sulfur (δ^{34}S) isotopes in bone collagen reflect those of the dietary protein consumed over the last few years of the animals life as bones slowly remodel (Ambrose and Norr, 1993; Hedges et al., 2007; Nehlich, 2015). By contrast, the tooth enamel oxygen (δ^{18}O) isotope signatures reflect the period over which the tooth mineralized, which for horse typically takes between 1.5 and 2.8 years, Stevens et al., 2009b depending on the tooth (Hoppe et al., 2004b).

Faunal δ^{13}C values are primarily determined by dietary ecology, reflecting the photosynthetic pathway at the base of the food chain. In Late Pleistocene Europe plants are thought to have almost exclusively used the C3 photosynthetic pathway (Ehleringer et al., 1997; Wiβing et al., 2016). Small-scale variation in C3 plant δ^{13}C values of the magnitude of a few ‰ is linked to vegetation type and a range of environmental parameters such as vegetation density (e.g. canopy effect, Drucker et al., 2008), ambient temperature, and water availability (Heaton, 1999; Dawson et al., 2003; Kohn, 2010). The δ^{13}C values of archaeological herbivore remains reflect their dietary choices and can reveal resource partitioning between individuals and species (Stevens et al., 2009b, 2025a; Britton et al., 2012; Schwartz-Narbonne et al., 2019).

Herbivore δ^{15}N values are primarily determined by the δ^{15}N values of plants at the base of the food chain. Plant δ^{15}N values reflect a complex interplay of various factors such as climate, plant functional type, mycorrhizal associations, soil characteristics, the availability of different forms of nitrogen and pathways of nitrogen uptake (Amundson et al., 2003; Craine et al., 2009, 2015; Hobbie and Högberg, 2012; Szpak, 2014). Archaeological herbivore δ^{15}N values have been used to reconstruct temporal changes in ecosystem baseline δ^{15}N values in response to climatic and environmental drivers (Richards and Hedges, 2003; Stevens and Hedges, 2004; Fox-Dobbs et al., 2008; Stevens et al., 2008; Bocherens et al., 2014; Reade et al., 2023), as a proxy for palaeoclimate and palaeoenvironmental reconstructions at archaeological sites, and to infer herbivore selective feeding and niche partitioning in ancient ecosystems (Stevens et al., 2009a, 2009b, 2014, 2025a; Britton et al., 2012, 2023; Jones et al., 2018, 2019; Schwartz-Narbonne et al., 2019; Reade et al., 2020a, 2020b, 2021).

Herbivore δ^{34}S values reflect the δ^{34}S values of plants consumed, which in turn reflect those of the bioavailable sulfur (usually soil sulfate). Bioavailable sulfur varies spatially, with isotope values being primarily determined by underlying bedrock and proximity to the ocean (due to sea spray) (Nehlich, 2015; Bataille et al., 2020; Guiry and Szpak, 2020). As there is little or no isotopic fraction with trophic level or due to physiology (Peterson et al., 1985; Krajcarz et al., 2019), archaeological faunal δ^{34}S values have been used to determine animal origin or mobility/migratory behaviours (Jones et al., 2018; Madgwick et al., 2019a, 2019b; Wiβing et al., 2019; Stevens et al., 2025a). However, there is increasing recognition that environmental parameters can influence bioavailable δ^{34}S values as soil-bedrock interactions, mineral weathering, and sulfur cycling in the soil are driven by hydrological and microbial processes (Thode and Krouse, 1991; Guiry et al., 2021; Stevens et al., 2022, 2025b). Diachronic changes and spatial trends in faunal δ^{34}S values in the late Pleistocene have been linked to climate/environmental conditions, in particular changing permafrost conditions, which impact soil and plant δ^{34}S values. This has been observed both within specific sites and across wide regions of Eurasia (Stevens et al., 2021, 2025b; Reade et al., 2020a, 2021). Thus, archaeological faunal δ^{34}S values can also provide information about the palaeoenvironment which humans were experiencing.

Oxygen isotopes (δ^{18}O) in herbivore tooth enamel reflect those of the ingested water consumed by the animal during the period of tooth formation (Luz and Kolodny, 1985; Hoppe et al., 2004a). In obligate drinkers, such as horses, ingested water closely mirrors precipitation δ^{18}O values. In mid to high latitudes where a strong linear relationship exists between precipitation δ^{18}O values and temperature, enamel δ^{18}O values can be used to reconstruct past air temperatures (Dansgaard, 1964; Kohn et al., 1996; Hoppe et al., 2004a; Kohn and Welker, 2005; Rozanski et al., 2013; Pryor et al., 2013). Enamel mineralizes progressively from the crown to the enamel–root junction and once mineralized does not remodel, thus preserving a time-sequence of seasonal isotopic variation (and temperature) that can be accessed through sequential sampling (Fricke and O'Neil, 1996; Sharp and Cerling, 1998).

2. Methods

Sixteen horse metapodial bones and three teeth were selected for this study from the Stránská skála IV material held at the Research Centre for Paleolithic and Paleoanthropology in Dolní Věstonice, Institute of Archaeology of the Czech Academy of Sciences, Brno. Given that the MNI for horses recovered from the site is 10, it is feasible that some individuals may have been sampled more than once. There was no visual evidence of the bones or teeth having been treated with a PVA glue consolidant. We also report here carbon isotope results for 39 collagen specimens from the Gravettian archaeological sites of Dolní Věstonice I (*Equus* n = 3, *Rangifer tarandus* n = 3) and Pavlov I (*Equus* n = 14, *Rangifer tarandus* n = 17) (held in the osteological collections of Budišov Castle), the Epigravettian sites of Brno-Štýřice III open air site (*Equus* n = 1) and the cave site of Býčí skála (*Rangifer tarandus* n = 1) (both held in the Moravian Museum, Brno)(see Supplementary information for further details). These sites are located in Moravia (Czech Republic) near to Stránská skála VI (Fig. 1) and provide comparative isotope data for discussion. Collagen extraction and analysis methods, along with nitrogen and sulfur isotope data for these samples have previously been published (Stevens et al., 2025b; Reade et al., 2023). In additions comparative faunal isotope data is available from the Gravettian site of Předmostí I (~31.5–29.5 ka cal. BP, Bocherens et al., 2015), and the Magdalenian (Layer 6–15.6–14.6 ka cal. BP), and Epimagdalenian (Layer 4, ~14.1–12.6 ka cal. BP) levels at Kůlna Cave (Reade et al., 2021) (Fig. 1).

2.1. Bone collagen extraction

Approximately 0.5g of bone was collected from each specimen using a dental drill with a small cutting wheel attachment. Collagen extraction was performed for 10 of the specimens at the University of Cambridge following a modified (Longin, 1971) method reported in (Stevens et al., 2008) and for 6 of the specimens at UCL Institute of Archaeology following a modified version of the Oxford Radiocarbon Accelerator Unit (ORAU) collagen extraction procedures (Brock et al., 2010), which is based on a modified version of the (Longin, 1971) method. The two methods only differ slightly. All samples were demineralized in 0.5 M aq. HCl at 4°C until they had fully demineralized. The samples prepared at UCL only, were then treated with 0.1 M sodium hydroxide (NaOH) for 30 mins to remove humic acids, before being thoroughly rinsed. All samples were then rinsed in ultrapure water and gelatinized by heating in pH 3.0 HCl aqueous solution at 75°C for 48h. The liquid fraction containing the dissolved collagen was filtered using a pre-cleaned Ezee-filter, frozen overnight at −20°C, then stored at −80°C for 4 h and finally lyophilized.

2.2. Radiocarbon analysis

After isotope analysis, 7 specimens were selected for radiocarbon dating. At UCL Institute of Archaeology the extracted collagen was rehydrated with ultrapure water and then passed through a pre-cleaned 15–30 kD ultrafilter, with the >30 kD fraction collected and freeze-dried. The ultra-filtered collagen was transferred to Oxford Radiocarbon Accelerator Unit for radiocarbon dating. Five mg of dry collagen was weighed into pre-baked tin capsules and combusted using an elemental analyser coupled to an isotope ratio mass spectrometer, employing a splitter to allow for collection of the CO_2 (Bronk Ramsey and Humm, 2000; Brock et al., 2010). Samples were graphitized by reduction of collected CO_2 over an iron catalyst in an excess H_2 atmosphere at 560°C (Bronk Ramsey and Hedges, 1997; Dee and Bronk Ramsey, 2000). ^{14}C dates were measured on the Oxford AMS system using a caesium ion source for ionization of the solid graphite sample (Ramsey et al., 2004b). Results are reported as uncalibrated radiocarbon dates (^{14}C BP) and discussed as calibrated dates BP (cal. BP). Date calibration was performed using OxCal 4.4 (Bronk Ramsey) and the INTCAL20 dataset (Reimer et al., 2020).

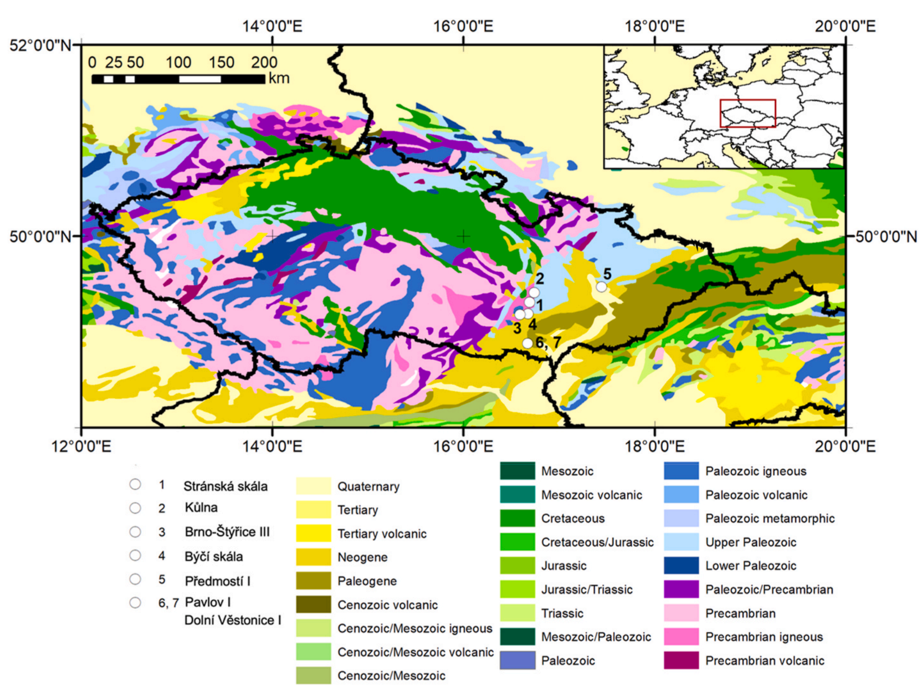

Fig. 1. Location of Moravian sites discussed in this study and underlying geology of the region.

2.3. Collagen stable isotope analysis

Bone collagen stable carbon ($\delta^{13}C$), nitrogen ($\delta^{15}N$), and sulfur ($\delta^{34}S$) isotopic ratios were determined on the extracted collagen of 15 samples using a Delta V Advantage continuous-flow isotope ratio mass spectrometer coupled via a ConfloIV to an IsoLink elemental analyser (Thermo Fisher Scientific, Bremen) at SUERC, University of Glasgow. Between 1.2 and 1.5 mg of collagen was loaded into a tin capsule for continuous flow combustion and isotopic analysis. Normalization was undertaken using one of two methods, either three in-house standards (SAG: $\delta^{15}N_{AIR} = 4.5 \pm 0.1$ ‰, $\delta^{13}C_{VPDB} = -13.8 \pm 0.1$ ‰, $\delta^{34}S_{VCTD} = -10.1 \pm 0.2$ ‰, MAG: $\delta^{15}N_{AIR} = 45.2 \pm 0.3$ ‰, $\delta^{13}C_{VPDB} = -24.9 \pm 0.1$ ‰, $\delta^{34}S_{VCTD} = 1.\ 6 \pm 0.2$ ‰ and MSAG: $\delta^{15}N_{AIR} = 3.9 \pm 0.3$ ‰, $\delta^{13}C_{VPDB} = -20.6 \pm 0.1$ ‰, $\delta^{34}S_{VCTD} = 10.8 \pm 0.1$ ‰), which were calibrated to the International Atomic Energy Agency (IAEA) reference materials USGS40 ($\delta^{15}N_{AIR} = -4.5 \pm 0.1$ ‰, $\delta^{13}C_{VPDB} = -26.4 \pm 0.04$ ‰), USGS41 ($\delta^{15}N_{AIR} = 47.6 \pm 0.2$ ‰, $\delta^{13}C_{VPDB} = 37.6 \pm 0.1$ ‰), USGS43 ($\delta^{15}N_{AIR} = 8.4 \pm 0.3$ ‰, $\delta^{13}C_{VPDB} = -21.3 \pm 0.1$ ‰, $\delta^{34}S_{VCTD} = 10.5 \pm 0.2$ ‰),IAEA-S-2 (silver sulfide, $\delta^{34}S_{VCTD} = 22.7 \pm 0.2$ ‰) and IAEA-S-3 (silver sulfide, $\delta^{34}S_{VCTD} = -32.3 \pm 0.2$ ‰), or they were normalized using USGS40, USGS41a ($\delta^{15}N_{AIR} = 47.6 \pm 0.2$ ‰, $\delta^{13}C_{VPDB} = 36.6 \pm 0.1$ ‰), and two in-house standards (SAG2B: $\delta^{34}S_{VCTD} = -9.2 \pm 0.1$ ‰ and MSAG2: $\delta^{34}S_{VCTD} = 11.3 \pm 0.1$ ‰) that were calibrated to IAEA-S-2 and IAEA-S-3.(Measurement uncertainty is ±0.1 ‰, ±0.2 ‰ and ±0.3 ‰ for $\delta^{13}C$, $\delta^{15}N$, and $\delta^{34}S$ values respectively, based on the repeat measurements of an in-house bone collagen standard (DHB2: $\delta^{15}N_{AIR} = 4.1 \pm 0.2$ ‰, $\delta^{13}C_{VPDB} = -21.0 \pm 0.1$ ‰, $\delta^{34}S_{VCTD} = 7.2 \pm 0.4$ ‰ or DHB2019: $\delta^{15}N_{AIR} = 3.7 \pm 0.1$ ‰, $\delta^{13}C_{VPDB} = -21.2 \pm 0.1$ ‰, $\delta^{34}S_{VCTD} = 9.4 \pm 0.4$ ‰) and a certified fish gelatin standard B2215 (Elemental Microanalysis, UK $\delta^{15}N_{AIR} = 4.3 \pm 0.1$ ‰, $\delta^{13}C_{VPDB} = -22.9 \pm 0.1$ ‰, $\delta^{34}S_{VCTD} = 1.2 \pm 0.2$ ‰).

Carbon ($\delta^{13}C$) and nitrogen ($\delta^{15}N$) isotopic ratios were determined for one sample at the Godwin Laboratory, University of Cambridge using an automated elemental analyser (Costech Analytical, Valencia, CA, USA) coupled in continuous-flow mode to a Thermo Finnigan MAT253 isotope ratio mass spectrometer (Thermo Fisher Scientific, Bremen, Germany). Between 0.6 and 1 mg of collagen was loaded into a tin capsule for isotopic analysis. International (IAEA: caffeine and glutamic acid-USGS-40) standards with known isotopic values and in-house laboratory standards (nylon, alanine and bovine liver standards) calibrated to the IAEA standards were interspersed throughout each analytical run and were used to normalize the collagen $\delta^{13}C$ and $\delta^{15}N$ values. Each sample was analysed in duplicate with analytical errors of ±0.2 ‰ for both $\delta^{13}C$ and $\delta^{15}N$ based on repeated measurements of calibration standards. All results are reported on the delta scale as per mil (‰) relative to the internationally accepted standards VPDB, AIR and VCDT.

2.4. Enamel pretreatment and isotope analysis

Sequential samples were taken from the enamel crowns of three horse teeth for carbonate stable oxygen ($\delta^{18}O$) isotope analysis. For each tooth, enamel samples were taken from the cusp that showed the best level of preservation. Tooth surfaces were cleaned with a brush and then lightly abraded using a tungsten drill bit. Powdered samples were collected during the drilling of sequential grooves perpendicular to the axis of growth. The intra-tooth enamel sample locations were measured relative to the enamel-root junction (ERJ). The collected enamel powder was prepared according to (Tornero et al., 2013). Samples were treated with 0.1 M acetic acid (0.1 ml/mg sample) for 4 hours, then thoroughly rinsed, frozen, and freeze dried. Enamel carbonate stable oxygen ($\delta^{18}O$) isotope analysis was performed at the Godwin Laboratory, Department of Earth Sciences, University of Cambridge. Enamel powder samples were reacted with 100 % orthophosphoric acid for 2h at 70°C in individual vessels either using a micromass multicarb sample preparation system followed by cryogenic transfer into a VG PRISM or VG SIRA isotope ratio mass spectrometer or using an automated cryogenic distillation system (Kiel III device), interfaced with a Finnigan MAT 253 isotope ratio mass spectrometer. The results are reported with reference to the international standard VPDB calibrated through the NBS19 standard (Coplen, 2011) for which the precision is better than ±0.11 ‰.

2.5. Statistical analyses

Statistical analyses and data visualization were performed using R software (*R version* 4.3.0)**.** Packages used include, tidyverse, dplyr, ggplot2, ggpmisc, gridExtra, openxlsx, cowplot, ggpubr, matrixcalc.f Statistical significance was tested using anova and pairwise t-tests.

3. Results

3.1. Radiocarbon

The seven new Stránská skála IV ultrafiltered AMS dates range from 24,120 to 23,250 cal. BP (Table 1). All seven new results provide dates that are older than the published dates from the site (Table 1, Fig. 2). Although small uncertainties are associated with the new radiocarbon dates, the calibrated age probability distributions are broad for some dates due to a plateau in the radiocarbon calibration curve (Supplementary Information Fig. 1). A Bayesian approach using OxCal (v.4.4) and the IntCal20 calibration curve was applied to the data. Four of the published dates were not included in the model (GrN-14351 and GrN-13954 as not ultrafiltered; DeA-20210 and DeA-20212 as known to have come from a tooth embedded in resin). Initially Poz-101463 was included in the model as it is uncertain whether this sample had been treated with a consolidant. However, our outlier analysis in OxCal showed this sample to be an outlier, and thus all older published dates were excluded. The results of the Bayesian modelling of the new AMS dates gives a boundary start date for the site of 24,170–23,780 cal. BP and a boundary end date of 23,740–23,080 cal. BP with a 95 % confidence interval (Fig. 3, Table 2). These results indicate the occupation of Stránská skála IV occurred before the brief GI-2 warm event recorded in the Greenland ice cores (Fig. 3).

3.2. Collagen C, N and S isotopes

Collagen was successfully extracted from all 56 samples. Standard quality control criteria were used to assess the $\delta^{13}C$, $\delta^{15}N$ and $\delta^{34}S$ data (DeNiro, 1985; Ambrose, 1990; Nehlich and Richards, 2009). All analysed samples passed these criteria having C:N atomic ratios between 3.2 and 3.6, and %C and %N of 13–44 % and 5–16 %, respectively, indicating good bone collagen preservation (DeNiro, 1985; Ambrose, 1990; Nehlich and Richards, 2009). All samples have C/S and N/S atomic ratios (369–821 and 113–242) within the recommended ranges of 600 ± 300 and 200 ± 100, and %S content between 0.12 and 0.27 % (Nehlich and Richards, 2009). The Stránská skála IV *Equus* bone collagen $\delta^{13}C$ values range from −20.1 ‰ to −19.7 ‰ ($n = 16$, Mean −20.1 ‰ $\sigma = 0.2$ ‰) (Fig. 4). Their $\delta^{15}N$ values range from 1.9 ‰ to 3.5 ‰ ($n = 16$, Mean 2.5 ‰, $\sigma = 0.5$ ‰) and their $\delta^{34}S$ values range from −13.4 ‰ to −2.8 ‰ ($n = 15$, Mean −7.5 ‰, $\sigma = 3.8$ ‰) (Fig. 4). The Dolní Věstonice *Equus* and *Rangifer* bone collagen $\delta^{13}C$ values range from −21.4 ‰ to −21.1 ‰ ($n = 3$, Mean −21.3 ‰, $\boldsymbol{\sigma} = 0.1$ ‰) and from −19.6 ‰ to −18.8 ‰ ($n = 3$, Mean −19.3 ‰, $\sigma = 0.4$ ‰) respectively (Fig. 5). The Pavlov *Equus* and *Rangifer* bone collagen $\delta^{13}C$ values range from −21.9 ‰ to −19.3 ‰ ($n = 13$, Mean −20.4 ‰, $\sigma = 1.1$ ‰) and from −20.5 ‰ to −18.5 ‰ ($n = 17$, Mean −20.2 ‰, $\sigma = 0.8$ ‰) respectively (Fig. 5). The Brno-Styrice III *Equus* bone collagen $\delta^{13}C$ value is −20.6 ‰, and the Byci Skala *Rangifer* $\delta^{13}C$ value is −19.6 ‰ (Fig. 5A).

3.3. Enamel O isotopes

Enamel $\delta^{18}O$ results are given in full in the Supplementary Data File and summarized in Table 3. Enamel $\delta^{18}O$ values ranged from 11.6 ‰ to

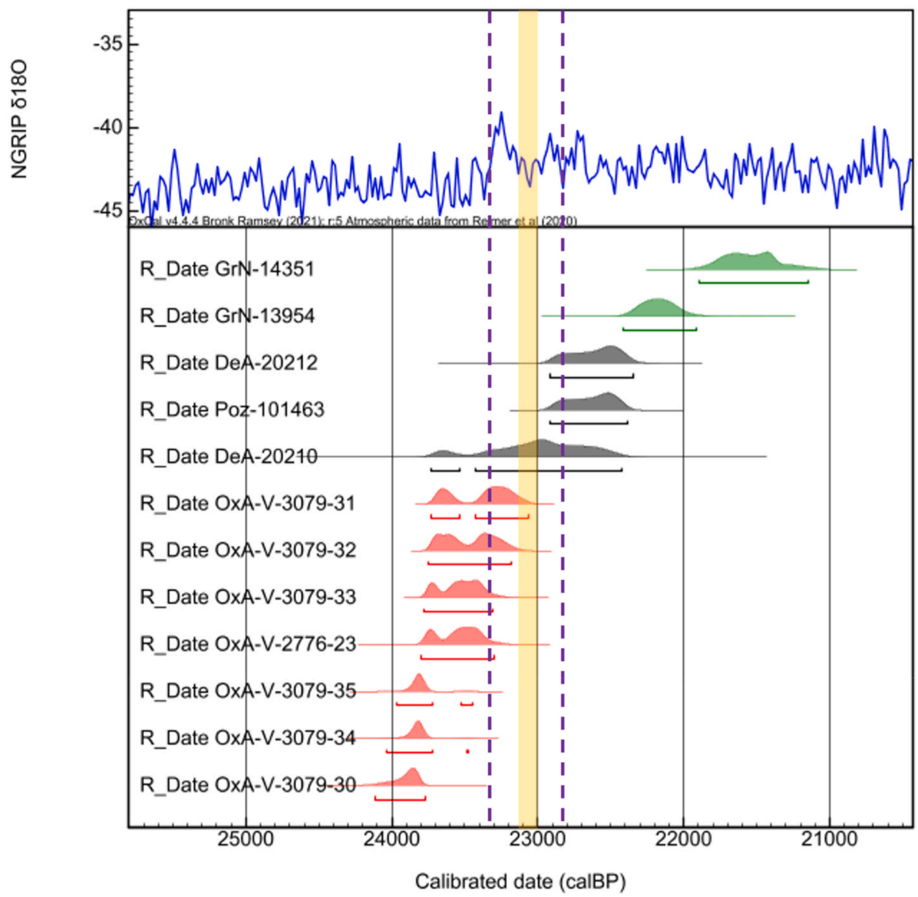

Fig. 2. Calibrated radiocarbon dates from Stránská skála IV. (Tables 1 and 2). Calibration performed using OxCal 4.4 and the INTCAL20 dataset and shown against the NGRIP δ^{18}O record (North Greenland Ice Core Project members, 2004). Green = previously published radiocarbon dates (not ultrafiltered), grey = previously published radiocarbon dates (ultrafiltered), red = new ultrafiltered AMS dates for this study. Dashed purple line indicates duration of Greenland Interstadial 2, which is intermediated by Greenland Stadial 2.2 (orange shading). (For interpretation of the references to colour in this figure legend, the reader is referred to the Web version of this article.)

16.2 ‰ (Mean 13.5 ‰ σ = 1.6 ‰) for SSK1, 11.0 ‰–13.9 ‰ (Mean 12.3 ‰ σ = 1.2 ‰) for SSK2, and 10.9 ‰–16.1 ‰ (Mean 12.3 ‰ σ = 1.7 ‰) for SSK3. Palaeo-drinking water δ^{18}O values and palaeotemperature estimates were then made for average (mid-point), winter (intra-tooth minima), and summer (intra-tooth maxima) δ^{18}O values. Enamel δ^{18}O results, which were measured on the carbonate phase on the enamel apatite, were first converted to the SMOW isotope scale (Coplen, 2011) and then their equivalent phosphate δ^{18}O value following (Bryant et al., 1996). The inverse model of (Passey et al., 2005), following the methodology of (Pederzani et al., 2021a), was then applied to the data to estimate the δ^{18}O value of the original input to the tooth, which becomes dampened by the process of mineralization and geometry of sampling. Inverse modelling was possible for two of our sampled teeth (SSK1, SSK2; Fig. 6, Table 3), but not possible for the third tooth (SSK3) as a sinusoidal pattern of isotopic variation, with a clear seasonal maxima and minima, was not observed in this tooth. The calculated summer high and winter lower δ^{18}O values for SSK1, SSK2, along with mid-point δ^{18}O values for all three teeth, were then used to estimate summer, winter and annual average paleotemperatures following methods in (Pryor et al., 2014) and using the empirical relationships defined between horse skeletal phosphate δ^{18}O and drinking water δ^{18}O by (Delgado Huertas et al., 1995) and between meteoric water δ^{18}O (taken to equivalate drinking water δ^{18}O) and air temperature by (Pryor et al., 2014). Further details of modelling and palaeotemperature calculations are given in the Supplementary Information. From this modelling, mean annual palaeo-drinking water δ^{18}O values was estimated to be −13.1 ‰ ± 1.7 ‰, with summer and winter values of −8.1 ‰ ± 1.8 ‰ and −16.3 ‰ ± 2.2 ‰, respectively (Supplementary Information Fig. 2). From this, the mean annual palaeotemperature of 1.2 ± 3.5°C is estimated, while summer and winter temperatures are estimated to be 10.7 ± 3.4°C and −4.9 ± 4.7°C, respectively (Fig. 7).

4. Discussion

The new radiocarbon evidence from the Stránská skála IV hunted horses indicates humans were present in Moravia during the LGM, between 24,110 and 23,140 cal. BP. This predates the brief GI-2 warm event recorded in the Greenland ice cores (23,290 ± 596 BP to 22,850 ± 573 BP (Rasmussen et al., 2014)). Whilst this correlation may suggest cold interglacial conditions at Stránská skála IV when humans were active at the site, the Greenland ice-core records are many thousands of kilometers from Moravia. Contemporaneous palaeoclimate data from Moravia is extremely limited. Thus, palaeoenvironmental information gained directly from the archaeological remains at Stránská skála IV is vital for gaining insight into the conditions experienced by the hunter-gatherers who created the site. The Stránská skála IV horse collagen δ^{13}C and δ^{15}N values are very uniform and are typical of other sites in Moravia dating to Oxygen Isotope Stage 2 (OIS-2, ~29–11.7 ka BP) (Fig. 5). The δ^{15}N values are comparable, but the δ^{13}C values are, whilst within the range of observed values (−21.3 to −19.2 ‰, n = 25), are skewed towards the higher end of the range (Iacumin et al., 1997; Drucker et al., 2000, 2003; Stevens and Hedges, 2004; Stevens, 2005; Higham et al., 2010; Domingo et al., 2015). Notably the Stránská skála IV δ^{13}C values are statistically significantly higher than those of horse

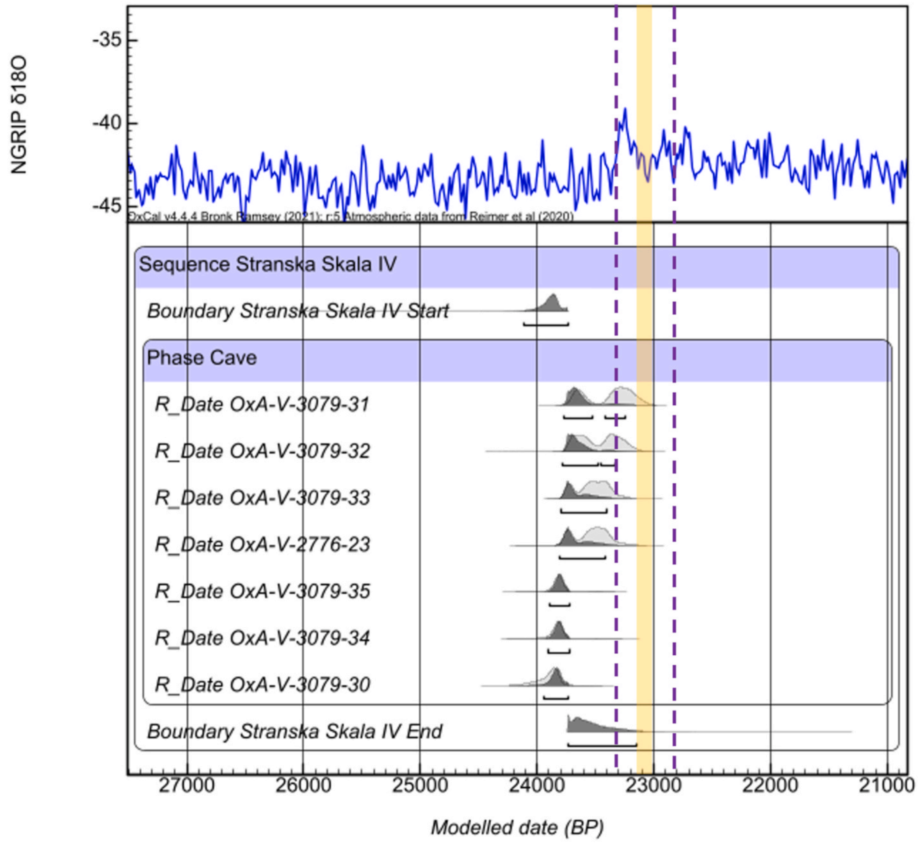

Fig. 3. Bayesian modeling of new ultrafiltered radiocarbon dates from Stránská skála IV. Calibration and modeling performed using OxCal 4.4 and the INTCAL20 dataset and shown against the NGRIP $\delta^{18}O$ record (North Greenland Ice Core Project members, 2004). Dashed purple line indicates duration of Greenland Interstadial 2, which is intermediated by Greenland Stadial 2.2 (orange shading). (For interpretation of the references to colour in this figure legend, the reader is referred to the Web version of this article.)

Table 2
New ultrafiltered radiocarbon dates from Stránská skála IV (This study) and results of Bayesian modelling using Boundary and Phase functions. Calibration and modelling performed using OxCal 4.4

	Unmodelled (BP)			Modelled (BP			Indices A_{model} = 101.8 $A_{overall}$ = 89				
	from	to	%	from	to	%	A_{comb}	A	L	P	C
Outlier_Model General				−270	410	95.4					100
T(5)	−2.65	2.65	95.4								99.7
U(0,4)	3.98986e-17	4	95.4	5.37764e-17	3.788	95.4		100			100
Sequence Stránská skála IV											
Boundary Stránská skála IV Start				24170	23780	95.4					99
Phase Cave											
R_Date OxA-V-3079-31	23740	23060	95.4	23770	23220	95.4		89.3		95.7	99.4
R_Date OxA-V-3079-32	23750	23170	95.4	23780	23310	95.4		105.3		96.1	99.3
R_Date OxA-V-3079-33	23790	23300	95.4	23800	23390	95.4		94.5		96.2	99.1
R_Date OxA-V-2776-23	23800	23300	95.4	23810	23390	95.4		94.8		96.3	99.1
R_Date OxA-V-3079-35	23980	23440	95.4	23920	23720	95.4		111.7		96.6	99.9
R_Date OxA-V-3079-34	24040	23470	95.4	23920	23730	95.4		112.5		96.5	99.9
R_Date OxA-V-3079-30	24120	23770	95.4	23970	23750	95.4		116.7		95.9	99.7
Span Stránská skála IV				70	660	95.4					99.8
Interval Stránská skála IV Int				70	1010	95.4					97.5
Boundary Stránská skála IV End				23740	23080	95.4					97.3

from both earlier and later sites in Moravia (Fig. 5A, see Supplementary Information for statistical tests), but are not statistically different to those at the LGM site of Kammern-Grubgraben (~24–20k cal. BP) located in Austria ~100 km southwest of Stránská skála (−20.8 ‰ to −19.4 ‰ (n = 13, Mean −20.4 ‰ σ = 0.4 ‰) (Reiss et al., 2023). However, the majority of the Kammern-Grubgraben horse $\delta^{13}C$ results are more negative than those of the Stránská skála horses (Fig. 8). Notably the Stránská skála horse $\delta^{13}C$ values overlap with those observed for OIS-2 reindeer from Moravia (−20.5 to −18.2 ‰, n = 37) (Fig. 5A). In reindeer, higher $\delta^{13}C$ values are linked to their consumption of lichens (Fizet et al., 1995; Stevens et al., 2009b; Drucker et al., 2011; Reade et al., 2020b), which have higher $\delta^{13}C$ values than other terrestrial plants from boreal ecosystems (Park and Epstein, 1960; Maguas and Brugnoli, 1996; Drucker et al., 2001). The Stránská skála IV horse $\delta^{13}C$

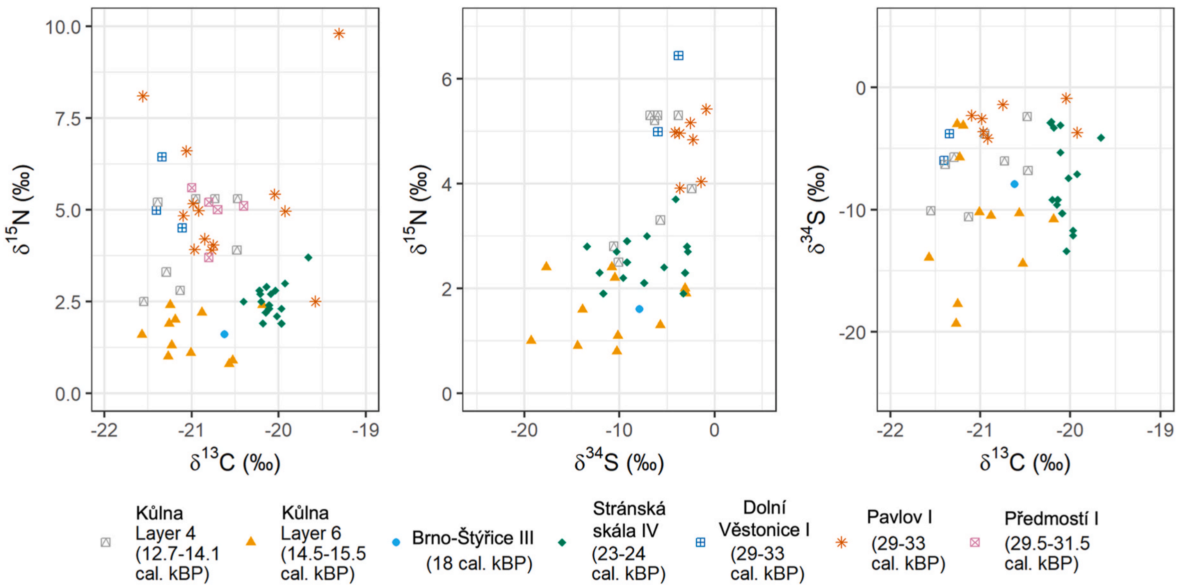

Fig. 4. Scatter plots of horse collagen δ^{13}C, δ^{15}N and δ^{34}S values from Stránská skála IV (This study), Pavlov, Dolní Věstonice, Brno-Štýřice III (δ^{13}C this study, δ^{15}N Reade et al., 2023; δ^{34}S Stevens et al., 2025b) Kůlna Cave (Reade et al., 2021), and Předmostí I (Bocherens et al., 2015).

values could indicate that the horse moved into the reindeer's ecological niche and consumed some lichen; however they are unlikely to have consumed enough for it to register in their bone collagen isotope values as horses are generalist grazers and in modern contexts do not selectively feed on lichen. It is more likely that the elevated horse δ^{13}C values reflect particularly arid conditions influencing the δ^{13}C values of plants consumed by the horses. As only horse isotope data is available from Stránská skála IV it is not possible at this time to determine whether aridity impacted on the isotopes of other species at this time.

Whilst the Stránská skála IV horse δ^{15}N values are comparable to those of OIS-2 horses from Western Europe (Reade et al., 2023), they significantly differ from earlier and later sites in Moravia (Fig. 5B, see Supplementary Information for statistical test). The temporal variation in horse δ^{15}N values in Moravia mirrors that observed in reindeer δ^{15}N values but is of a greater magnitude (Fig. 5B). As with carbon isotopes, this difference between species is linked to reindeer consuming lichen, which fixes nitrogen from the atmosphere, and therefore has δ^{15}N values that are decoupled from environmentally-mediated changes in vegetation δ^{15}N (Reade et al., 2023), whereas horses are not buffered in this way. Temporal excursions in late Pleistocene faunal δ^{15}N values are widely observed across Northwest and Central Europe (Drucker et al., 2003; Richards and Hedges, 2003; Hedges et al., 2004; Stevens and Hedges, 2004; Stevens, 2005; Stevens et al., 2008, 2014; Bocherens et al., 2014; Rabanus-Wallace et al., 2017; Reade et al., 2020a, 2023), with higher δ^{15}N values observed in OIS3, a switch to lower δ^{15}N values during OIS2, and the lowest δ^{15}N values being observed at the end of the Pleniglacial (Greenland Stadial 2.1) prior to the Late Glacial (Greenland interstadial 1e-a) when nitrogen began to rebound to higher values (Reade et al., 2023). These changes in faunal δ^{15}N values reflect a complex interplay of multiple environmental parameters impacting on soil, plant, and thus faunal δ^{15}N values. The lowest δ^{15}N values appear to be reserved for regions that were glaciated or where continuous permafrost existed at the height of the Last Glacial Maximum, and occur only after the onset of deglaciation and thaw. Thus increased landscape moisture, particularly from ice sheet meltwater and thawing permafrost has long been suggested as a driver of low post-LGM δ^{15}N values (Stevens and Hedges, 2004; Stevens et al., 2008; Drucker et al., 2009; Reade et al., 2023). In Moravia the switch from higher horse δ^{15}N values prior to 29 ka cal. BP to lower δ^{15}N at Stránská skála IV 24-23 ka cal. BP coincides with the suspected timing of regional permafrost development (Vandenberghe and Pissart, 1993; Vandenberghe et al., 2014); is consistent with the horse δ^{13}C values which indicate increased aridity; and with palaeoclimate data which indicates prevailing cold arid desert conditions in central Europe (Römer et al., 2016; Fuhrmann et al., 2020; Sirocko et al., 2022). A single horse from Brno Štýřice and a reindeer from Býčí skála Cave dating to the start of the post-LGM period have lower δ^{15}N values than the Stránská skála IV horses, thus the pattern of late Pleistocene faunal nitrogen change in Moravia appears fully consistent with that seen elsewhere in Europe. The Stránská skála IV overlap with but are mostly slightly higher than those of the Kammern-Grubgraben horses (Reiss et al., 2023) (Fig. 8). Given the regional trends in δ^{15}N this may suggest the Kammern-Grubgraben horses cover a longer time period, and perhaps partially post-date those from Stránská skála IV, which is consistent with the radiocarbon dates from the two site.

The Stránská skála IV horse δ^{34}S values are more variable than their δ^{13}C and δ^{15}N values (Figs. 4 and 5C). The δ^{34}S values are comparable to those of other OIS-2 herbivores from areas of West and Central Europe where continuous permafrost existed during the LGM, but are lower than those of herbivores from regions where permafrost was absent during the LGM (Stevens et al., 2025b). The Stránská skála IV horse δ^{34}S values fit into a temporal trend observed in horses and other species from Moravia (Fig. 5C). Prior to 29 ka BP herbivore δ^{34}S values are high (but note that some species partitioning exists within sites that are likely linked to differing home ranges). The most notable difference between the Stránská skála IV horse δ^{34}S values and Moravian fauna from earlier periods is the increased range in δ^{34}S and the presence of low δ^{34}S values. Like with δ^{15}N values, the lowest δ^{34}S values are observed after the LGM at Kůlna Cave layer 6 which dates to the end of the Pleniglacial (Greenland stadial 2.1). The herbivore δ^{34}S values rebound to higher values during the Late Glacial (Kůlna layer 4). This Late Pleniglacial Sulfur Excursion (LPSE) has been observed in faunal δ^{34}S values across large regions of Eurasia and is likely linked to changing permafrost conditions affecting hydrological processes, rates of weathering of sulfides and sulfide oxidation, and microbial activity in periodically waterlogged, anoxic soils, in addition to loess deposition, which in turn impact terrestrial sulfur cycling (Stevens et al., 2025b). Thus the change in both faunal δ^{15}N and δ^{34}S values in Moravia between c. 29 ka cal. BP and c. 24-23 ka cal. BP indicate a substantial change in both the nitrogen and sulfur biogeochemical cycles at this time which likely relates to the development of permafrost.

Palaeotemperature reconstructions based on the horse intra-tooth

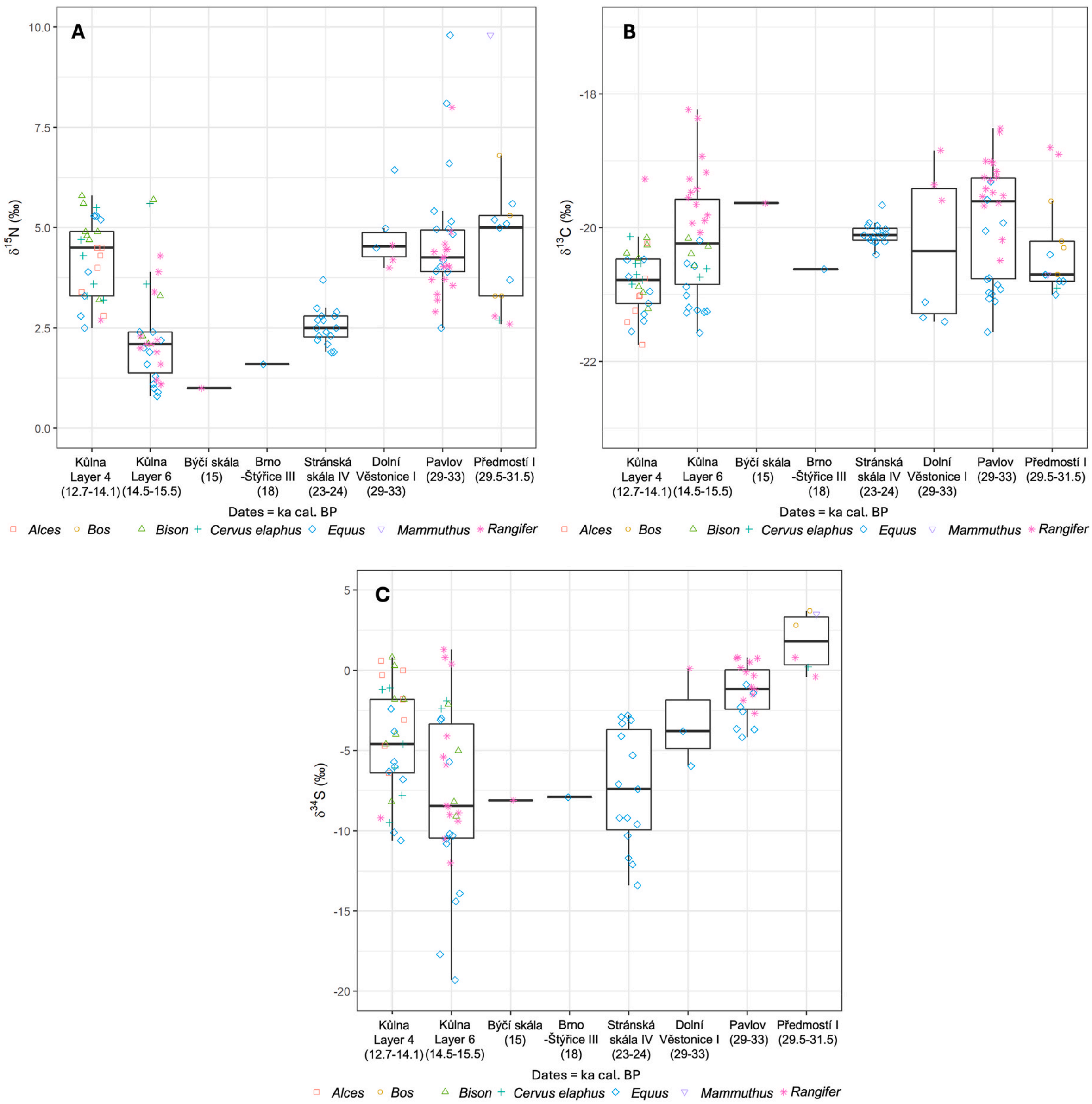

Fig. 5. Box plot of faunal collagen A) $\delta^{13}C$, B) $\delta^{15}N$ and C) $\delta^{34}S$ values from Stránská skála IV (This study), Pavlov, Dolní Věstonice, Brno-Štýřice III and Býčí skála ($\delta^{13}C$ this study, $\delta^{15}N$ Reade et al., 2023; $\delta^{34}S$ Stevens et al., 2025b) Kůlna Cave (Reade et al., 2021), and Předmostí I (Bocherens et al., 2015).

Table 3
Summary statistic for enamel phosphate $\delta^{18}O$ (SMOW) isotope results (see Supplementary Information for conversion from measured carbonate V-PDB).

Tooth number	Mean	Standard deviation	Median	Min	Max	Midpoint
SSK1	13.5	1.6	13.4	11.6	16.2	13.9
SSK2	12.3	1.2	11.8	11.0	13.9	12.4
SSK3	12.3	1.7	11.5	10.9	16.1	13.5

enamel $\delta^{18}O$ values indicate that conditions at Stránská skála IV were considerably colder than the present day, with summer temperature around 10° lower but winter temperatures only around 3° lower (Fig. 7; Supplementary Information section 3). It should however be noted that considerable uncertainty exists in the palaeotemperature estimates due to the small number of used and the necessity of using modern temperature-$\delta^{18}O_{precipitation}$ data to generate the estimates. The mean annual palaeotemperature estimates presented here from incrementally-sampled teeth (1.2 ± 3.5°C) closely match those from bulk tooth enamel $\delta^{18}O$ analysis of horse from Stránská skála IV (n = 12, Pryor, 2011) and from climate simulations (Fig. 7, Beyer et al., 2020). Mean annual palaeotemperature estimates (−3.5 ± 2.9 °C) from incrementally-sampled horse teeth at the LGM site of Kammern-Grubgraben indicate slightly cooler conditions (Reiss et al., 2024) than those at Stránská skála IV. The intra-tooth Stránská skála IV enamel $\delta^{18}O$-based estimated summer temperatures (10.7 ± 3.4 °C) are broadly consistent with those based on the Kammern-Grubgraben intra-tooth enamel $\delta^{18}O$ (8.0 ± 3.9 °C to 11.4 ± 3.7 °C) whereas the estimated winter temperatures are substantially higher (−4.9 ± 4.7 °C) compared to those estimated for Kammern-Grubgraben (−24.3 ± 6.4 °C to −9.9 ± 4.3 °C). This disparity between the two likely reflect greater seasonality at Kammern-Grubgraben compared to Stránská skála IV and is potentially due to chronological differences between the two sites. The Stránská skála IV intra-tooth enamel $\delta^{18}O$-based estimated summer temperatures are lower, and estimated winter temperatures are higher, respectively, than those from climate simulations (Fig. 7, Beyer et al., 2020). Seasonal palaeotemperature reconstructions from incrementally sampled enamel are especially complex due to the necessity of using an

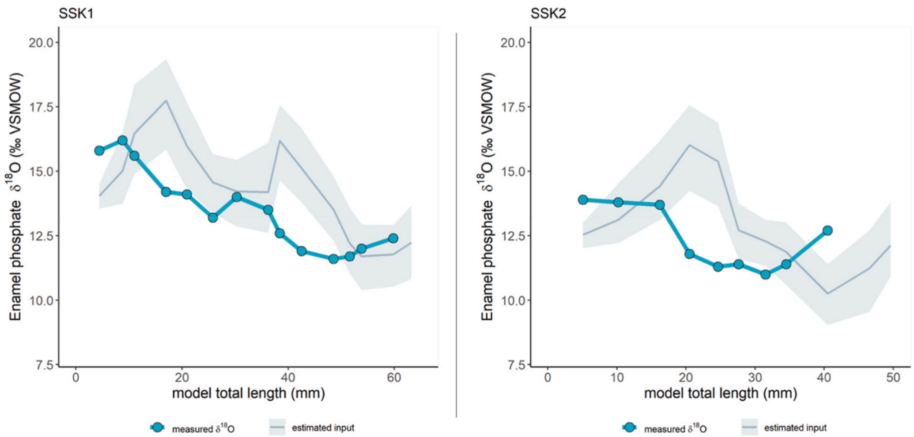

Fig. 6. Measured oxygen isotope values ($\delta^{18}O$ enamel; blue dots) for two *Equus* teeth, and inverse modelled isotopic input (grey line) with 95 % confidence interval (grey shaded area) based on Passey et al., (2005). (For interpretation of the references to colour in this figure legend, the reader is referred to the Web version of this article.)

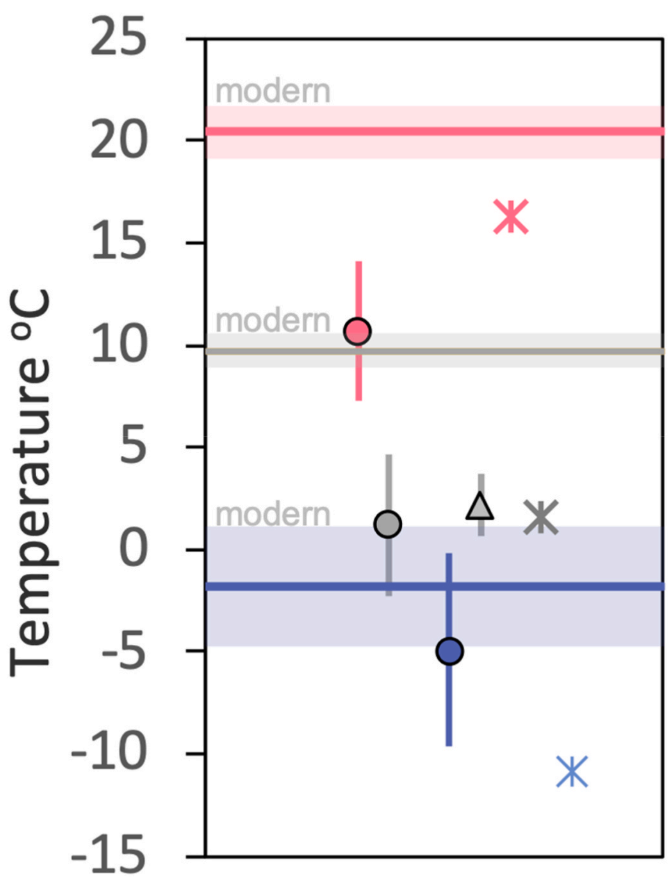

Fig. 7. Estimated average annual (grey), summer (pink), and winter (blue) paleotemperatures based on 1) Stránská skála IV horse intra-tooth $\delta^{18}O$ enamel carbonate data (circles) 2) Stránská skála IV bulk horse tooth $\delta^{18}O$ enamel carbonate data (triangle; n = 12: Pryor, 2011) and 3) on the 24,000 interval of the 0.5° resolution, biased-corrected combined HadCM3 and HadAM3H time series climate simulations (Crosses) (Beyer et al., 2020). For 1 and 2 associated compound errors are shown as error bars. Lines represent modern temperatures for Stránská skála's location, with associated standard deviations shown as shaded ribbons. Modern temperature data were obtained from the ClimateEU model and averaged for 1991 to 2020 (Marchi et al., 2020). (For interpretation of the references to colour in this figure legend, the reader is referred to the Web version of this article.)

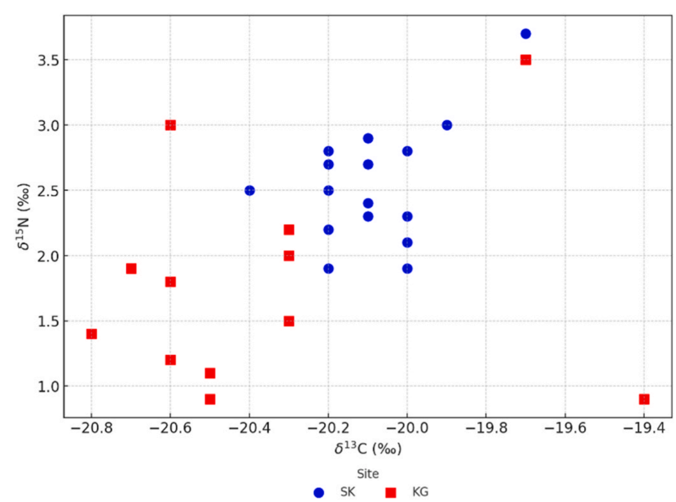

Fig. 8. Scatter plots of horse collagen $\delta^{13}C$ and $\delta^{15}N$ from the Last Glacial Maximum sites of Stránská skála IV (SS) (This study) and Kammern-Grubgraben (KG) (Reiss et al., 2023).

inverse model to remove the impact of time averaging from the tooth enamel mineralization (Passey et al., 2005). Here, either the climate simulations are over-estimating the temperature seasonality in the Stránská skála IV region or the enamel-based seasonal palaeotemperature reconstructions are underestimating temperature seasonality, or both. The potentially attenuated seasonality in the enamel based seasonal palaeotemperature reconstructions could be linked to uncertainties with the modelling variables used here to generate the estimated inputs, or to the Passey model not fully removing the impact of time averaging introduced during enamel mineralization. Alternatively, it could be that the Stránská skála IV horse's drinking water $\delta^{18}O$ values were seasonally buffered through the horse consuming water from rivers or springfed groundwater. Notably a palaeochannel of the Svitava river is proximal to the site, indicating that such a water source could have been accessed by the horses.

5. Conclusions

Our program of radiocarbon dating of hunted horse remains from Stránská skála IV and Bayesian modelling show humans were active at the site between 24.1 and 23 ka cal. BP. This predates the GI-2 brief warm event (c. 23.3–22.8 ka BP) recorded in Greenland ice-cores

(Rasmussen et al., 2014). Through correlating the chronology of the Stránská skála IV occupation and the Greenland ice-core stratigraphy (a global temperature proxy record), we can speculate that cold stadial conditions prevailed at Stránská skála IV. On-site palaeoclimatic reconstructions based on carbon, nitrogen, sulfur and oxygen isotope analysis of hunted horse remains show that local climate and environmental conditions were consistent with those suggested by correlation with global climate records. The bone collagen $\delta^{13}C$, $\delta^{15}N$ and $\delta^{34}S$ data indicate conditions were cool and arid with an open landscape, which was likely being impacted by changes in hydrology linked to permafrost development. The enamel $\delta^{18}O$ data indicates mean annual air temperatures of 1.2 °C (±3.5 °C), consistent with climate simulations-based temperature estimates for the region during the LGM. Together these data indicate humans were present at the site during pronounced cold conditions characterized by temperatures ~8.5°C below the modern-day average. These data help to further understand the limited pollen data from the site. Interpreting the thermophilic elements of the pollen data as representing warm conditions at the site is at odds with all the other palaeoenvironmental reconstructions. Other interpretations of the thermophilic elements of the pollen data, such as it representing: 1) small relic populations surviving locally under cold continental climate conditions; 2) long distance transport of pollen from strong pollen producers living in warmer regions; or, 3) pollen reworked from older or younger deposits are all consistent with the new palaeoenvironmental reconstructions (Svoboda et al., 2020). Our results are consistent with evidence from Kammern-Grubgraben (Reiss et al., 2024) in demonstrating that human presence in central Europe during the LGM was not confined to brief warm events, necessitating a rethinking of the climate conditions early humans could tolerate at the edge of their home ranges. This adds to a growing body of evidence that at certain times in prehistory, climate played a less deterministic role in human distribution than previously thought.

CRediT authorship contribution statement

Rhiannon E. Stevens: Writing – review & editing, Writing – original draft, Visualization, Project administration, Methodology, Investigation, Funding acquisition, Formal analysis, Data curation, Conceptualization. **Hazel Reade:** Writing – review & editing, Visualization, Methodology, Investigation, Formal analysis, Data curation. **Alexander J.E. Pryor:** Writing – review & editing, Methodology, Investigation, Conceptualization. **Kerry L. Sayle:** Writing – review & editing, Methodology, Formal analysis. **Jennifer A. Tripp:** Writing – review & editing, Investigation, Formal analysis. **Petr Neruda:** Writing – review & editing, Investigation, Formal analysis. **Zdeňka Nerudová:** Writing – review & editing, Investigation, Formal analysis. **Martina Roblíčková:** Writing – review & editing, Methodology, Investigation, Conceptualization. **Thomas Higham:** Methodology, Investigation, Funding acquisition. **Jiří Svoboda:** Writing – review & editing, Investigation, Formal analysis.

Declaration of competing interest

The authors declare the following financial interests/personal relationships which may be considered as potential competing interests: Rhiannon Stevens reports financial support was provided by The Royal Society. Rhiannon Stevens reports financial support was provided by European Research Council. If there are other authors, they declare that they have no known competing financial interests or personal relationships that could have appeared to influence the work reported in this paper.

Acknowledgements

This research was funded by the European Research Council (Consolidator grant to RS: ERC-CG-617777: UP-North) and the Royal Society (Fellowship to RS: 502008.K518/SLB). We thank the Research Centre for Paleolithic and Paleoanthropology in Dolní Věstonice, Institute of Archaeology of the Czech Academy of Sciences for allowing access to material. György Lengyel, Mihaly Molnar, and Sandra Sázelová are thanked for providing information on previous analyses of Stránská skála IV material. Tamsin O'Connell and Martin Jones are thanked for useful discussions and advice.

Appendix A. Supplementary data

Supplementary data to this article can be found online at https://doi.org/10.1016/j.quaint.2025.109893.

References

Ambrose, S.H., 1990. Preparation and characterization of bone and tooth collagen for isotopic analysis. J. Archaeol. Sci. https://doi.org/10.1016/0305-4403(90)90007-r.

Ambrose, S.H., Norr, L., 1993. Experimental evidence for the relationship of the carbon isotope ratios of whole diet and dietary protein to those of bone collagen and carbonate. In: Lambert, J.B., Grupe, G. (Eds.), Prehistoric Human Bone: Archaeology at the Molecular Level. Springer Berlin Heidelberg, Berlin, Heidelberg, pp. 1–37.

Amundson, R., Austin, A.T., Schuur, E.A.G., Yoo, K., Matzek, V., Kendall, C., Uebersax, A., Brenner, D., Baisden, W.T., 2003. Global patterns of the isotopic composition of soil and plant nitrogen. Glob. Biogeochem. Cycles 17. https://doi.org/10.1029/2002gb001903.

Bataille, C.P., Chartrand, M.M.G., Raposo, F., St-Jean, G., 2020. Assessing geographic controls of hair isotopic variability in human populations: a case-study in Canada. PLoS One 15, e0237105.

Beyer, R.M., Krapp, M., Manica, A., 2020. High-resolution terrestrial climate, bioclimate and vegetation for the last 120,000 years. Sci. Data 7, 236.

Bocherens, H., Drucker, D.G., Madelaine, S., 2014. Evidence for a $^{(15)}N$ positive excursion in terrestrial foodwebs at the middle to upper Palaeolithic transition in south-western France: implications for early modern human palaeodiet and palaeoenvironment. J. Hum. Evol. 69, 31–43.

Bocherens, H., Drucker, D.G., Germonpré, M., Lázničková-Galetová, M., Naito, Y.I., Wissing, C., Brůžek, J., Oliva, M., 2015. Reconstruction of the Gravettian food-web at Předmostí I using multi-isotopic tracking (^{13}C, ^{15}N, ^{34}S) of bone collagen. Quat. Int. 359–360, 211–228.

Boriová, S., Sázelová, S., Novák, M., Štelcl, J., Svoboda, J., 2020. Human and non-human taphonomic effects on faunal remains from the Late Upper Paleolithic: a case study from the Stránská skála IV site, Czech Republic. Int. J. Osteoarchaeol. 30, 155–169.

Britton, K., Gaudzinski-Windheuser, S., Roebroeks, W., Kindler, L., Richards, M.P., 2012. Stable isotope analysis of well-preserved 120,000-year-old herbivore bone collagen from the middle Palaeolithic site of neumark-nord 2, Germany reveals niche separation between bovids and equids. Palaeogeogr. Palaeoclimatol. Palaeoecol. 333, 168–177.

Britton, K., Jimenez, E.-L., Le Corre, M., Pederzani, S., Daujeard, C., Jaouen, K., Vettese, D., Tütken, T., Hublin, J.-J., Moncel, M.-H., 2023. Multi-isotope zooarchaeological investigations at Abri du Maras: the paleoecological and paleoenvironmental context of Neanderthal subsistence strategies in the Rhône Valley during MIS 3. J. Hum. Evol. 174, 103292.

Brock, F., Higham, T., Ditchfield, P., Ramsey, C.B., 2010. Current pretreatment methods for AMS radiocarbon dating at the Oxford Radiocarbon Accelerator Unit (ORAU). Radiocarbon 52, 103–112.

Bronk Ramsey, C., n.d. Oxcal Version 4.4 Oxford: Radiocarbon Accelerator Unit. University of Oxford.

Bronk Ramsey, C., Hedges, R.E.M., 1997. Hybrid ion sources: radiocarbon measurements from microgram to milligram. Nucl. Instrum. Methods Phys. Res., Sect. B 123, 539–545.

Bronk Ramsey, C., Humm, M.J., 2000. On-line combustion of samples for AMS and ion source developments at ORAU. Nucl. Instrum. Methods Phys. Res., Sect. B 172, 242–246.

Bryant, D.J., Koch, P.L., Froelich, P.N., Showers, W.J., Genna, B.J., 1996. Oxygen isotope partitioning between phosphate and carbonate in Mammalian apatite. Geochem. Cosmochim. Acta 60, 5145–5148.

Clark, P.U., Dyke, A.S., Shakun, J.D., Carlson, A.E., Clark, J., Wohlfarth, B., Mitrovica, J. X., Hostetler, S.W., McCabe, A.M., 2009. The Last Glacial Maximum. Science 325, 710–714.

Coplen, T.B., 2011. Guidelines and recommended terms for expression of stable-isotope-ratio and gas-ratio measurement results. Rapid Commun. Mass Spectrom.: RCM (Rapid Commun. Mass Spectrom.) 25, 2538–2560.

Craine, J.M., Elmore, A.J., Aidar, M.P.M., Bustamante, M., Dawson, T.E., Hobbie, E.A., Kahmen, A., Mack, M.C., McLauchlan, K.K., Michelsen, A., Nardoto, G.B., Pardo, L. H., Peñuelas, J., Reich, P.B., Schuur, E.A.G., Stock, W.D., Templer, P.H., Virginia, R. A., Welker, J.M., Wright, I.J., 2009. Global patterns of foliar nitrogen isotopes and their relationships with climate, mycorrhizal fungi, foliar nutrient concentrations, and nitrogen availability. New Phytol. 183, 980–992.

Craine, J.M., Brookshire, E.N.J., Cramer, M.D., Hasselquist, N.J., Koba, K., Marin-Spiotta, E., Wang, L., 2015. Ecological interpretations of nitrogen isotope ratios of terrestrial plants and soils. Plant Soil 396, 1–26.

Dansgaard, W., 1964. Stable Isotopes in Precipitation, vol. 16. Tell'Us, pp. 436–468.

Dawson, T.E., Mambelli, S., Plamboeck, A.H., Templer, P.H., Tu, K.P., 2003. Stable isotopes in. Plant Ecol. https://doi.org/10.1146/annurev.ecolsys.33.020602.095451.

Dee, M., Bronk Ramsey, C., 2000. Refinement of graphite target production at ORAU. Nucl. Instrum. Methods Phys. Res., Sect. B 172, 449–453.

Delgado Huertas, A., Iacumin, P., Stenni, B., Sánchez Chillón, B., Longinelli, A., 1995. Oxygen isotope variations of phosphate in Mammalian bone and tooth enamel. Geochem. Cosmochim. Acta 59, 4299–4305.

DeNiro, M.J., 1985. Postmortem preservation and alteration of in vivo bone collagen isotope ratios in relation to palaeodietary reconstruction. Nature 317, 806–809.

Domingo, L., Pérez-Dios, P., Hernández Fernández, M., Martín-Chivelet, J., Ortiz, J.E., Torres, T., 2015. Late Quaternary climatic and environmental conditions of northern Spain: an isotopic approach based on the mammalian record from La Paloma cave. Palaeogeogr. Palaeoclimatol. Palaeoecol. 440, 417–430.

Drucker, D., Bocherens, H., Cleyet-Merle, J.-J., Madelaine, S., Mariotti, A., 2000. Implications paléoenvironnementales de l'étude isotopique (^{13}C, ^{15}N) de la faune des grands mammifères des Jamblancs (Dordogne, France)/Isotopic study (^{13}C, ^{15}N) of large mammal fauna from Les Jamblancs (Dordogne, France): paleoenvironnemental implications. Paléo, Revue d'Archéologie Préhistorique 12, 127–140.

Drucker, D., Bocherens, H., Pike-Tay, A., Mariotti, A., 2001. Isotopic tracking of seasonal dietary change in dentine collagen: preliminary data from modern caribou. Comptes Rendus Acad. Sci. - Ser. IIA Earth Planet. Sci. 333, 303–309.

Drucker, D.G., Bocherens, H., Billiou, D., 2003. Evidence for shifting environmental conditions in Southwestern France from 33 000 to 15 000 years ago derived from carbon-13 and nitrogen-15 natural abundances in collagen of large herbivores. Earth Planet Sci. Lett. 216, 163–173.

Drucker, D.G., Bridault, A., Hobson, K.A., Szuma, E., Bocherens, H., 2008. Can carbon-13 in large herbivores reflect the canopy effect in temperate and boreal ecosystems? Evidence from modern and ancient ungulates. Palaeogeogr. Palaeoclimatol. Palaeoecol. 266, 69–82. https://doi.org/10.1016/j.palaeo.2008.03.020.

Drucker, D.G., Bridault, A., Iacumin, P., Bocherens, H., 2009. Bone stable isotopic signatures (^{15}N,^{18}O) as tracers of temperature variation during the late-glacial and early Holocene: case study on red deerCervus elaphusfrom rochedane (jura, France). Geol. J. 44, 593–604.

Drucker, D.G., Kind, C.-J., Stephan, E., 2011. Chronological and ecological information on late-glacial and early Holocene reindeer from northwest Europe using radiocarbon (^{14}C) and stable isotope (^{13}C, ^{15}N) analysis of bone collagen: case study in Southwestern Germany. Quat. Int.: the journal of the International Union for Quaternary Research 245, 218–224.

Drucker, D.G., Stevens, R.E., Germonpré, M., Sablin, M.V., Péan, S., Bocherens, H., 2018. The end of the mammoth steppe in central East European plains during the Epigravettian: insights from collagen stable isotopes. Quat. Res. 90, 457–469.

Ehleringer, J.R., Cerling, T.E., Helliker, B.R., 1997. C4 photosynthesis, atmospheric CO_2, and climate. Oecologia 112, 285–299.

Ehlers, J., Gibbard, P.L., 2013. Glaciations: overview. Encyclopedia Quater. Sci. https://doi.org/10.1016/b978-0-444-53643-3.00128-x.

Fizet, M., Mariotti, A., Bocherens, H., Lange-Badré, B., Vandermeersch, B., Borel, J.P., Bellon, G., 1995. Effect of diet, physiology and climate on carbon and nitrogen stable isotopes of collagen in a late Pleistocene anthropic palaeoecosystem: Marillac, Charente, France. J. Archaeol. Sci. 22, 67–79.

Fox-Dobbs, K., Leonard, J.A., Koch, P.L., 2008. Pleistocene megafauna from eastern beringia: paleoecological and paleoenvironmental interpretations of stable carbon and nitrogen isotope and radiocarbon records. Palaeogeogr. Palaeoclimatol. Palaeoecol. 261, 30–46.

Fricke, H.C., O'Neil, J.R., 1996. Inter- and intra-tooth variation in the oxygen isotope composition of Mammalian tooth enamel phosphate: implications for palaeoclimatological and palaeobiological research. Palaeogeogr. Palaeoclimatol. Palaeoecol. https://doi.org/10.1016/s0031-0182(96)00072-7.

Fuhrmann, F., Diensberg, B., Gong, X., Lohmann, G., Sirocko, F., 2020. Aridity synthesis for eight selected key regions of the global climate system during the last 60 000 years. Clim. Past 16, 2221–2238.

Gamble, C., Davies, W., Pettitt, P., Richards, M., 2004. Climate change and evolving human diversity in Europe during the last glacial. Phil. Trans. Roy. Soc. Lond. B Biol. Sci. 359, 243–253. ; discussion 253–4.

Guiry, E., Noël, S., Fowler, J., 2021. Archaeological herbivore δ^{13}C and δ^{34}S provide a marker for saltmarsh use and new insights into the process of 15N-enrichment in coastal plants. J. Archaeol. Sci. 125, 105295.

Guiry, E.J., Szpak, P., 2020. Seaweed-eating sheep show that δ^{34}S evidence for marine diets can be fully masked by sea spray effects. Rapid Commun. Mass Spectrom.: RCM (Rapid Commun. Mass Spectrom.) 34, e8868.

Haesaerts, P., Damblon, F., Neugebauer-Maresch, C., Einwögerer, T., 2016. Radiocarbon chronology of the late Palaeolithic loess site of Kammern-Grubgraben (lower Austria). Archaeol. Austriaca 100, 271–277.

Heaton, T.H.E., 1999. Spatial, species, and temporal variations in the ^{13}C/^{12}C ratios of C3 plants: implications for palaeodiet studies. J. Archaeol. Sci. 26, 637–649.

Hedges, R.E.M., Stevens, R.E., Richards, M.P., 2004. Bone as a stable isotope archive for local climatic information. Quat. Sci. Rev. 23, 959–965.

Hedges, R.E.M., Clement, J.G., Thomas, C.D.L., O'Connell, T.C., 2007. Collagen turnover in the adult femoral mid-shaft: modeled from anthropogenic radiocarbon tracer measurements. Am. J. Phys. Anthropol. 133, 808–816.

Heyman, B.M., Heyman, J., Fickert, T., Harbor, J.M., 2013. Paleo-climate of the central European uplands during the last glacial maximum based on glacier mass-balance modeling. Quat. Res. 79, 49–54.

Higham, T., Jacobi, R., Julien, M., David, F., Basell, L., Wood, R., Davies, W., Ramsey, C. B., 2010. Chronology of the Grotte du Renne (France) and implications for the context of ornaments and human remains within the Châtelperronian. Proc. Natl. Acad. Sci. U. S. A 107, 20234–20239.

Higham, T.F.G., Jacobi, R.M., Bronk Ramsey, C., 2006. AMS radiocarbon dating of ancient bone using ultrafiltration. Radiocarbon 48, 179–195.

Hobbie, E.A., Högberg, P., 2012. Nitrogen isotopes link mycorrhizal fungi and plants to nitrogen dynamics. New Phytol. 196, 367–382.

Hoppe, K.A., Amundson, R., Vavra, M., McClaran, M.P., Anderson, D.L., 2004a. Isotopic analysis of tooth enamel carbonate from modern North American feral horses: implications for paleoenvironmental reconstructions. Palaeogeogr. Palaeoclimatol. Palaeoecol. 203, 299–311.

Hoppe, K.A., Stover, S.M., Pascoe, J.R., Amundson, R., 2004b. Tooth enamel biomineralization in extant horses: implications for isotopic microsampling. Palaeogeogr. Palaeoclimatol. Palaeoecol. 206, 355–365.

Iacumin, P., Bocherens, H., Delgado Huertas, A., Mariotti, A., Longinelli, A., 1997. A stable isotope study of fossil mammal remains from the Paglicci Cave, southern Italy. N and C as palaeoenvironmental indicators. Earth Planet Sci. Lett. 148, 349–357.

Jankovská, V., Pokorný, P., 2008. Forest vegetation of the last full-glacial period in the Western carpathians (slovakia and Czech Republic). Preslia 80, 307–324.

Jones, J.R., Richards, M.P., Straus, L.G., Reade, H., Altuna, J., Mariezkurrena, K., Marín-Arroyo, A.B., 2018. Changing environments during the middle-upper Palaeolithic transition in the eastern cantabrian region (spain): direct evidence from stable isotope studies on ungulate bones. Sci. Rep. 8, 14842.

Jones, J.R., Richards, M.P., Reade, H., Quirós, F.B. de, Marín-Arroyo, A.B., 2019. Multi-isotope investigations of ungulate bones and teeth from El castillo and covalejos caves (cantabria, Spain): implications for paleoenvironment reconstructions across the middle-upper Palaeolithic transition. J. Archaeol. Sci.: Report 23, 1029–1042.

Klein, K., Wegener, C., Schmidt, I., Rostami, M., Ludwig, P., Ulbrich, S., Richter, J., Weniger, G.-C., Shao, Y., 2021. Human existence potential in Europe during the Last Glacial Maximum. Quat. Int.: the journal of the International Union for Quaternary Research 581–582, 7–27.

Kohn, M.J., 2010. Carbon Isotope Compositions of Terrestrial C3 Plants as Indicators of (Paleo)Ecology and (Paleo)Climate, 107. Proceedings of the National Academy of Sciences, pp. 19691–19695.

Kohn, M.J., Welker, J.M., 2005. On the temperature correlation of δ^{18}O in modern precipitation. Earth Planet Sci. Lett. 231, 87–96.

Kohn, M.J., Schoeninger, M.J., Valley, J.W., 1996. Herbivore tooth oxygen isotope compositions: effects of diet and physiology. Geochem. Cosmochim. Acta 60, 3889–3896.

Krajcarz, M.T., Krajcarz, M., Drucker, D.G., Bocherens, H., 2019. Prey-to-fox isotopic enrichment of ^{34}S in bone collagen: implications for paleoecological studies. Rapid Commun. Mass Spectrom.: RCM (Rapid Commun. Mass Spectrom.) 33, 1311–1317.

Lengyel, G., Bárány, A., Béres, S., Cserpák, F., Gasparik, M., Major, I., Molnár, M., Nadachowski, A., Nemergut, A., Svoboda, J., Verpoorte, A., Wojtal, P., Wilczyński, J., 2021. The Epigravettian chronology and the human population of eastern central Europe during MIS2. Quat. Sci. Rev. 271, 107187.

Longin, R., 1971. New method of collagen extraction for radiocarbon dating. Nature 230, 241–242.

Luz, B., Kolodny, Y., 1985. Oxygen isotope variations in phosphate of biogenic apatites, IV. Mammal teeth and bones. Earth Planet Sci. Lett. 75, 29–36.

Madgwick, R., Grimes, V., Lamb, A.L., Nederbragt, A.J., Evans, J.A., McCormick, F., 2019a. Feasting and mobility in Iron Age Ireland: multi-Isotope analysis reveals the vast catchment of navan fort, Ulster. Sci. Rep. 9, 19792.

Madgwick, R., Lamb, A.L., Sloane, H., Nederbragt, A.J., Albarella, U., Pearson, M.P., Evans, J.A., 2019b. Multi-isotope analysis reveals that feasts in the Stonehenge environs and across Wessex drew people and animals from throughout Britain. Sci. Adv. 5, eaau6078.

Maguas, C., Brugnoli, E., 1996. Spatial variation in carbon isotope discrimination across the thalli of several lichen species. Plant Cell Environ. 19, 437–446.

Maier, A., Lehmkuhl, F., Ludwig, P., Melles, M., Schmidt, I., Shao, Y., Zeeden, C., Zimmermann, A., 2016. Demographic estimates of hunter–gatherers during the Last Glacial Maximum in Europe against the background of palaeoenvironmental data. Quat. Int.: the journal of the International Union for Quaternary Research 425, 49–61.

Marchi, M., Castellanos-Acuña, D., Hamann, A., Wang, T., Ray, D., Menzel, A., 2020. ClimateEU, scale-free climate normals, historical time series, and future projections for Europe. Sci. Data 7, 428.

Nehlich, O., 2015. The application of sulphur isotope analyses in archaeological research: a review. Earth Sci. Rev. https://doi.org/10.1016/j.earscirev.2014.12.002.

Nehlich, O., Richards, M.P., 2009. Establishing collagen quality criteria for sulphur isotope analysis of archaeological bone collagen. Archaeol. Anthropol. Sci. 1, 59–75.

Nerudová, Z., Doláková, N., Novák, J., 2016. New information augmenting the picture of local environment at the LGM/LGT in the context of the middle danube region. Holocene 26, 1345–1354.

North Greenland Ice Core Project members, 2004. High-resolution record of northern hemisphere climate extending into the last interglacial period. Nature 431, 147–151.

Novák, J., Trotsiuk, V., Sýkora, O., Svoboda, M., Chytrý, M., 2014. Ecology of *Tilia sibirica* in a Continental hemiboreal forest, southern siberia: an analogue of a glacial refugium of broad-leaved temperate trees? Holocene. https://doi.org/10.1177/0959683614534744.

Park, R., Epstein, S., 1960. Carbon isotope fractionation during photosynthesis. Geochem. Cosmochim. Acta 21, 110–126.

Passey, B.H., Cerling, T.E., Schuster, G.T., Robinson, T.F., Roeder, B.L., Krueger, S.K., 2005. Inverse methods for estimating primary input signals from time-averaged isotope profiles. Geochem. Cosmochim. Acta 69, 4101–4116.

Pederzani, S., Aldeias, V., Dibble, H.L., Goldberg, P., Hublin, J.-J., Madelaine, S., McPherron, S.P., Sandgathe, D., Steele, T.E., Turq, A., Britton, K., 2021a. Reconstructing Late Pleistocene paleoclimate at the scale of human behavior: an example from the Neandertal occupation of La Ferrassie (France). Sci. Rep. 11, 1419.

Pederzani, S., Britton, K., Aldeias, V., Bourgon, N., Fewlass, H., Lauer, T., McPherron, S.P., Rezek, Z., Sirakov, N., Smith, G.M., Spasov, R., Tran, N.-H., Tsanova, T., Hublin, J.-J., 2021b. Subarctic climate for the earliest Homo sapiens in Europe. Sci. Adv. 7, eabi4642.

Peterson, B.J., Howarth, R.W., Garritt, R.H., 1985. Multiple stable isotopes used to trace the flow of organic matter in estuarine food webs. Science 227, 1361–1363.

Pryor, A.J.E., 2011. Humans and the Dansgaard-Oeschger Cycles in Northern Europe 50,000-20,000ya. University of Cambridge.

Pryor, A.J.E., O'Connell, T.C., Wojtal, P., Krzemińska, A., Stevens, R.E., 2013. Investigating climate at the upper Palaeolithic site of kraków spadzista street (B), Poland, using oxygen isotopes. Quat. Int. 294, 108–119.

Pryor, A.J.E., Stevens, R.E., O'Connell, T.C., Lister, J.R., 2014. Quantification and propagation of errors when converting vertebrate biomineral oxygen isotope data to temperature for palaeoclimate reconstruction. Palaeogeogr. Palaeoclimatol. Palaeoecol. 412, 99–107.

Pryor, A.J.E., Nesnídalová, T., Šída, P., Lengyel, G., Standish, C.D., Milton, J.A., Cooper, M.J., Hambach, B., Crowley, J., Wilczyński, J., 2024. Reindeer prey mobility and seasonal hunting strategies in the late Gravettian mammoth steppe. Archaeol. Anthropol. Sci. 16, 1–22.

Rabanus-Wallace, M.T., Wooller, M.J., Zazula, G.D., Shute, E., Jahren, A.H., Kosintsev, P., Burns, J.A., Breen, J., Llamas, B., Cooper, A., 2017. Megafaunal isotopes reveal role of increased moisture on rangeland during late Pleistocene extinctions. Nature ecology evolution 1, 125.

Ramsey, C.B., Higham, T., Bowles, A., Hedges, R., 2004a. Improvements to the pretreatment of bone at Oxford. Radiocarbon 46, 155–163.

Ramsey, C.B., Higham, T., Leach, P., 2004b. Towards high-precision AMS: progress and limitations. Radiocarbon 46, 17–24.

Rasmussen, S.O., Bigler, M., Blockley, S.P., Blunier, T., Buchardt, S.L., Clausen, H.B., Cvijanovic, I., Dahl-Jensen, D., Johnsen, S.J., Fischer, H., Gkinis, V., Guillevic, M., Hoek, W.Z., Lowe, J.J., Pedro, J.B., Popp, T., Seierstad, I.K., Steffensen, J.P., Svensson, A.M., Vallelonga, P., Vinther, B.M., Walker, M.J.C., Wheatley, J.J., Winstrup, M., 2014. A stratigraphic framework for abrupt climatic changes during the last glacial period based on three synchronized Greenland ice-core records: refining and extending the INTIMATE event stratigraphy. Quat. Sci. Rev. 106, 14–28.

Reade, H., O'Connell, T.C., Barker, G., Stevens, R.E., 2016. Pleistocene and Holocene palaeoclimates in the Gebel Akhdar (Libya) estimated using herbivore tooth enamel oxygen isotope compositions. Quat. Int.: the journal of the International Union for Quaternary Research 404, 150–162.

Reade, H., Tripp, J.A., Charlton, S., Grimm, S.B., Leesch, D., Müller, W., Sayle, K.L., Fensome, A., Higham, T.F.G., Barnes, I., Stevens, R.E., 2020a. Deglacial landscapes and the Late Upper Palaeolithic of Switzerland. Quat. Sci. Rev. 239, 106372.

Reade, H., Tripp, J.A., Charlton, S., Grimm, S., Sayle, K.L., Fensome, A., Higham, T.F.G., Barnes, I., Stevens, R.E., 2020b. Radiocarbon chronology and environmental context of Last Glacial Maximum human occupation in Switzerland. Sci. Rep. 10, 4694.

Reade, H., Grimm, S.B., Tripp, J.A., Neruda, P., Nerudová, Z., Roblíčková, M., Sayle, K.L., Kearney, R., Brown, S., Douka, K., Higham, T.F.G., Stevens, R.E., 2021. Magdalenian and Epimagdalenian chronology and palaeoenvironments at Kůlna Cave, moravia, Czech Republic. Archaeol. Anthropol. Sci. 13, 4.

Reade, H., Tripp, J.A., Frémondeau, D., Sayle, K.L., Higham, T.F.G., Street, M., Stevens, R.E., 2023. Nitrogen palaeo-isoscapes: changing spatial gradients of faunal δ^{15}N in late Pleistocene and early Holocene Europe. PLoS One, 0268607.

Reimer, P.J., Austin, W.E.N., Bard, E., Bayliss, A., Blackwell, P.G., Bronk Ramsey, C., Butzin, M., Cheng, H., Edwards, L.R., Friedrich, M., Grootes, P.M., Guilderson, T.P., Hajdas, I., Heaton, T.J., Hogg, A.G., Hughen, K.A., Kromer, B., Manning, S.W., Muscheler, R., Palmer, J.G., Pearson, C., van der Plicht, J., Reimer, R.W., Richards, D.A., Marian Scott, E., Southon, J.R., Turney, C.S.M., Wacker, L., Adolphi, F., Büntgen, U., Capano, M., Fahrni, S.M., Fogtmann-Schulz, A., Friedrich, R., Köhler, P., Kudsk, S., Miyake, F., Olsen, J., Reinig, F., Sakamoto, M., Sookdeo, A., Talamo, S., 2020. The IntCal20 northern hemisphere radiocarbon age calibration curve (0–55 cal kBP). Radiocarbon 62, 725–757.

Reiss, L., Mayr, C., Pasda, K., Einwögerer, T., Händel, M., Lücke, A., Maier, A., Wissel, H., 2023. Changing food webs before and during the Last Glacial Maximum based on stable isotopes of animal bone collagen from Lower Austria. J. Quat. Sci. 38, 1337–1356. https://doi.org/10.1002/jqs.3552.

Reiss, L., Mayr, C., Pasda, K., Joachimski, M.M., Einwögerer, T., Händel, M., Maier, A., 2024. Seasonal climate variations during marine isotope stages 3 and 2 inferred from high-resolution oxygen isotope ratios in horse tooth enamel from Lower Austria. J. Quat. Sci. 39, 531–546. https://doi.org/10.1002/jqs.3613.

Richards, M.P., Hedges, R.E.M., 2003. Variations in bone collagen δ^{13}C and δ^{15}N values of fauna from northwest Europe over the last 40 000 years. Palaeogeogr. Palaeoclimatol. Palaeoecol. 193, 261–267.

Römer, W., Lehmkuhl, F., Sirocko, F., 2016. Late Pleistocene aeolian dust provenances and wind direction changes reconstructed by heavy mineral analysis of the sediments of the Dehner dry maar (Eifel, Germany). Global Planet. Change 147, 25–39.

Rozanski, K., Araguás-Araguás, L., Gonfiantini, R., 2013. Isotopic patterns in modern global precipitation. In: Climate Change in Continental Isotopic Records. American Geophysical Union, Washington, D. C., pp. 1–36

Schwartz-Narbonne, R., Longstaffe, F.J., Kardynal, K.J., Druckenmiller, P., Hobson, K.A., Jass, C.N., Metcalfe, J.Z., Zazula, G., 2019. Reframing the mammoth steppe: insights from analysis of isotopic niches. Quat. Sci. Rev. 215, 1–21.

Sharp, Z.D., Cerling, T.E., 1998. Fossil isotope records of seasonal climate and ecology: straight from the horse's mouth. Geology 26, 219–222.

Sirocko, F., Albert, J., Britzius, S., Dreher, F., Martínez-García, A., Dosseto, A., Burger, J., Terberger, T., Haug, G., 2022. Thresholds for the presence of glacial megafauna in central Europe during the last 60,000 years. Sci. Rep. 12, 20055.

Škrdla, P., Vlach, M., Nejman, L., Bartík, J., Demidenko, Y.E., Rychtaříková, T., 2021. Settlement strategies in eastern central Europe during the maximum extent of the last glacial ice sheet. Quat. Int.: the journal of the International Union for Quaternary Research 581–582, 164–174.

Stevens, R.E., Pederzani, S., Britton, K., Wexler, S.K., 2025a. In press. Bones and teeth isotopes as archives for palaeoclimatic, palaeoenvironmental and palaeoecological data. Quat. Sci. Rev. 357, 109320.

Stevens, R.E., Reade, H., Sayle, K., Tripp, J., Frémondeau, D., Lister, A., Barnes, I., Germonpré, M., Street, M., Murton, J., Bottrell, S., Higham, T., 2025b. Major Excursions in Sulfur Isotopes Linked to Permafrost Change in Eurasia During the Last 50,000 Years. Nature Geosciences (in press).

Stevens, R.E., 2005. Establishing Links Between climate/environment & Both Modern & Archaeological Hair & Bone Isotope Values : Determining the Potential of Archaeological Bone Collagen δ^{13}C and δ^{15}N as Palaeoclimatic and Palaeoenvironmental Proxies. University of Oxford.

Stevens, R.E., Hedges, R., 2004. Carbon and nitrogen stable isotope analysis of northwest European horse bone and tooth collagen, 40,000 BP–present: palaeoclimatic interpretations. Quat. Sci. Rev. 23 (7–8), 977–991.

Stevens, R.E., Jacobi, R., Street, M., Germonpré, M., Conard, N.J., Münzel, S.C., Hedges, R.E.M., 2008. Nitrogen isotope analyses of reindeer (*Rangifer tarandus*), 45,000 BP to 9,000 BP: palaeoenvironmental reconstructions. Palaeogeogr. Palaeoclimatol. Palaeoecol. 262, 32–45.

Stevens, R.E., Germonpré, M., Petrie, C.A., O'Connell, T.C., 2009a. Palaeoenvironmental and chronological investigations of the Magdalenian sites of Goyet Cave and Trou de Chaleux (Belgium), via stable isotope and radiocarbon analyses of horse skeletal remains. J. Archaeol. Sci. 36, 653–662.

Stevens, R.E., O'Connell, T.C., Hedges, R.E.M., Street, M., 2009b. Radiocarbon and stable isotope investigations at the central Rhineland sites of Gönnersdorf and Andernach-Martinsberg, Germany. J. Hum. Evol. 57, 131–148.

Stevens, R.E., Hermoso-Buxán, X.L., Marín-Arroyo, A.B., Gonzalez-Morales, M.R., Straus, L.G., 2014. Investigation of late Pleistocene and early Holocene palaeoenvironmental change at El Mirón cave (Cantabria, Spain): insights from carbon and nitrogen isotope analyses of Red Deer. Palaeogeogr. Palaeoclimatol. Palaeoecol. 414, 46–60.

Stevens, R.E., Reade, H., Read, D.S., Bottrell, S.H., Frémondeau, D., Wexler, S., 2022. Iso-wetlands: unlocking wetland ecologies and agriculture in prehistory through sulfur isotopes. Archaeol. Int. 25 (11). https://doi.org/10.14324/111.444.ai.2022.

Stevens, R.E., Reade, H., Tripp, J., Sayle, K.A., Walker, E.A., 2021. Changing environment at the Late Upper Palaeolithic site of Lynx Cave, north Wales. In: Saudzinski-Windheuser J.O., S. (Ed.), The Beef Behind all Possible Pasts. the Tandem-Festschrift in Honour of Elaine Turner and Martin Street. Römisch-Germanischen Zentralmuseums, pp. 589–607.

Strandberg, G., Brandefelt, J., KjellströM, E., Smith, B., 2011. High-resolution regional simulation of Last Glacial Maximum climate in Europe. Tellus. Series A, Dynamic Meteorol. Oceanogr. 63, 107–125.

Svoboda, J., 1990. Moravia during the upper pleniglacial. In: Soffer, O., Gamble, C. (Eds.), The World at 18000BP: Volume One, High Latitudes.

Svoboda, J., Jelínek, S., Ložek, V., Mook, W.G., Peške, L., Přichystal, A., 1991. Stránská skála. Výsledky výzkumu v letech 1985-1987. Památky archeologické 82, 5–47.

Svoboda, J., Boriová, S., Lengyel, G., Pokorný, P., Přichystal, A., Sázelová, S., Wilczyński, J., 2020. Last glacial maximum landscape and Epigravettian horse hunting strategy in central Europe: the case of stránská skála IV. Přehled výzkumů 59–70.

Szpak, P., 2014. Complexities of nitrogen isotope biogeochemistry in plant-soil systems: implications for the study of ancient agricultural and animal management practices. Front. Plant Sci. 5, 288.

Terberger, T., 2013. Le Dernier Maximum glaciaire entre le Rhin et le Danube, un réexamen critique. Mémoire de la Société préhistorique française 56, 415–443.

Terberger, T., Street, M., 2002. Hiatus or continuity? New results for the question of pleniglacial settlement in central Europe. Antiquity 76, 691–698.

Thode, 1991. Sulphur isotopes in nature and the environment: an overview. In: Krouse, H.R., G.V, A. (Eds.), Stable Isotopes: Natural and Anthropogenic Sulfur in the Environment. John Wiley & Sons., New York, pp. 1–21.

Tornero, C., Bălăşescu, A., Ughetto-Monfrin, J., Voinea, V., Balasse, M., 2013. Seasonality and season of birth in early eneolithic sheep from Cheia (Romania): methodological advances and implications for animal economy. J. Archaeol. Sci. 40, 4039–4055.

Vandenberghe, J., Pissart, A., 1993. Permafrost changes in Europe during the last glacial. Permafr. Periglac. Process. 4, 121–135.

Vandenberghe, J., French, H.M., Gorbunov, A., Marchenko, S., Velichko, A.A., Jin, H., Cui, Z., Zhang, T., Wan, X., 2014. The last permafrost maximum (LPM) map of the northern hemisphere: permafrost extent and mean annual air temperatures, 25-17 ka BP. Boreas 43, 652–666.

Verpoorte, A., 2004. Eastern central Europe during the pleniglacial. Antiquity 78, 257–266.

Wißing, C., Rougier, H., Crevecoeur, I., Germonpré, M., Naito, Y.I., Semal, P., Bocherens, H., 2016. Isotopic evidence for dietary ecology of late neandertals in north-western Europe. Quat. Int.: the journal of the International Union for Quaternary Research 411, 327–345.

Wißing, C., Rougier, H., Baumann, C., Comeyne, A., Crevecoeur, I., Drucker, D.G., Gaudzinski-Windheuser, S., Germonpré, M., Gómez-Olivencia, A., Krause, J., Matthies, T., Naito, Y.I., Posth, C., Semal, P., Street, M., Bocherens, H., 2019. Stable isotopes reveal patterns of diet and mobility in the last neandertals and first modern humans in Europe. Sci. Rep. 9, 4433.